



Faculty of Science and Technology

MASTER'S THESIS

| | |
|--|---|
| Study program/ Specialization: Petroleum Engineering Drilling Engineering | Spring semester, 2013 Open access |
| Writer: Bjørn Skjerve | (Writer's signature) |
| Faculty supervisor: External supervisor(s): | Professor Helge Hodne Dr. Tor Henry Omland (Statoil) |
| Title of thesis: Experimental Investigation of the Potential of UCA and NMR for the Detection of Particle Sedimentation in Drilling Fluids | |
| Credits (ECTS): 30 sp | |
| Key words: Barite Sag Drilling Fluid NMR UCA OWR Micronized Particles | Pages: 40 + enclosure: 15 Stavanger, June 17 th /2013 Date/year |

til Vilde

Abstract

Both ultrasound and Nuclear Magnetic Resonance (NMR) have previously been investigated for the potential of monitoring barite sag in drilling fluids. The Ultrasonic Cement Analyzer (UCA) registers the speed of ultrasound waves travelling through a media, which is dependent on the speed of sound of the base fluid, density stratification, particle concentration, shape and size. The NMR measures the longitudinal and transverse relaxation time of the fluid, being dependent on three relaxation mechanisms. These are bulk relaxation, depending upon physical properties such as viscosity; surface relaxation, that accounts for the effect of contact between fluid and solids; and relaxation due to molecular diffusion.

An experimental study has been performed with the aim to investigate the ability of these two apparatus to detect sag in low sag potential drilling fluids with micronized barite. Experiments have been carried out on four different oil water ratios. Direct weight measurement has been performed using a modified atmospheric consistometer, in order to evaluate the behavior of the particles in the drilling fluid at a static condition.

Comparison of the results from the UCA and the NMR with the direct weight measurement have indicated possibilities and restrictions in the use of these two methods.

The UCA has showed potential in detecting accumulation of particles, as sediment beds are formed at the bottom of the test cell. A clear trend with an increasing transit time was indicated to take place after accumulation of approximately 3 grams of particles.

1D profile experiments performed by the use of a bench-top NMR spectrometer have shown potential in detecting sediment accumulation at the bottom of fluid samples. However, it seems like this test method may have a limited sensitivity restricting the gain in applying this test method on low sag potential drilling fluids.

It has been observed that transverse relaxation time, T_2 , changes with changing oil water ratio. As the number of signal peaks and their placement on the axis representing the relaxation time are probably representing hydrogen nuclei in different structural configurations, this measurement technique might also be applicable in emulsion stability analysis.

Acknowledgement

I would like to thank Professor Helge Hodne, my academic supervisor at the University of Stavanger. His support and patience have been outstanding and very helpful. Professor Ola Ketil Siqveland at the University of Stavanger has offered his help in the NMR lab, of which I am grateful.

I would like to thank my technical advisor Dr. Tor Henry Omland, Leading Advisor Drilling Fluids Department in Statoil, for making the arrangements needed to fulfill this work and making it an interesting project. I would also like to address a few words of thanks to M.Sc Tomasz Wroblewski, Engineer Drilling Technology, Statoil, for his support both in the laboratory work, and for reading the proofs of my thesis and for his guidance in technical issues.

Halliburton has provided mud recipes and ingredients for this project. A special thanks to Hege Anita Handeland Nilsen, Team Leader Baroid Lab, Halliburton, for making the deliveries and providing me with training in the laboratory.

A thanks to fellow student Øyvind Vestrheim for assistance, discussions and sharing of the laboratory equipment.

I would like to thank my parents for their support during all of my years of studying.

At last, I would like to thank my wonderful wife Siri for her love and support. This would not have been possible without her caring and patience.

Stavanger, June 2013

Bjørn Skjerve

Table of contents

| | |
|--|----|
| Abstract | 3 |
| Acknowledgement | 4 |
| Table of contents | 5 |
| 1. Introduction | 7 |
| 2. Theory | 8 |
| 2.1. Barite sag | 8 |
| 2.2. Settling kinetics | 8 |
| 2.2.1. Hindered settling | 8 |
| 2.2.2. Boycott effect | 9 |
| 2.3. Stokes law | 9 |
| 2.4. Rheological properties influence on sag | 10 |
| 2.5. Micronized weight particles | 10 |
| 2.6. Sag determination techniques | 10 |
| 2.6.1. Static sag testing | 10 |
| 2.6.2. Viscometer dynamic sag testing | 11 |
| 2.6.3. Sag flow loop | 11 |
| 2.6.4. High Angle Sag Test Device | 12 |
| 2.6.5. Direct weight measurement | 12 |
| 2.6.6. Ultrasonic measurements for sag detection | 12 |
| 2.6.7. Sag detection using NMR | 13 |
| 2.6.7.1. NMR measurement principle | 13 |
| 2.6.7.2. Relaxation mechanisms | 14 |
| 3. Experimental Work | 15 |
| 3.1. Mixing procedures | 16 |
| 3.1.1. UIS mud | 16 |
| 3.1.1.1. WBM | 16 |
| 3.1.1.2. OBM | 16 |
| 3.1.2. Halliburton OBM | 17 |
| 3.2. Mud composition | 17 |
| 3.2.1. UIS WBM | 17 |
| 3.2.2. UIS OBM | 17 |
| 3.2.3. Halliburton OBM | 17 |
| 3.3. Test equipment | 18 |
| 3.3.1. Direct Weight Measurement | 18 |
| 3.3.2. UCA | 19 |
| 3.3.3. NMR | 19 |
| 3.4. Test procedures | 20 |
| 4. Results | 21 |
| 4.1. UIS WBM | 21 |
| 4.1.1. Direct Weight Measurement | 21 |

| | |
|--|----|
| 4.1.2. UCA | 21 |
| 4.2. UIS OBM | 22 |
| 4.3. Halliburton OBM | 22 |
| 4.3.1. OWR 70/30 | 22 |
| 4.3.1.1. Direct Weight Measurement | 22 |
| 4.3.1.2. UCA | 23 |
| 4.3.1.3. NMR | 24 |
| 4.3.1.3.1. 1D Profile | 24 |
| 4.3.1.3.2. T2 | 24 |
| 4.3.2. OWR 75/25 | 25 |
| 4.3.2.1. Direct Weight Measurement | 25 |
| 4.3.2.2. UCA | 26 |
| 4.3.2.3. NMR | 26 |
| 4.3.2.3.1. 1D Profile | 26 |
| 4.3.2.3.2. T2 | 27 |
| 4.3.3. OWR 80/20 | 28 |
| 4.3.3.1. Direct Weight Measurement | 28 |
| 4.3.3.2. UCA | 28 |
| 4.3.3.3. NMR | 29 |
| 4.3.3.3.1. 1D Profile | 29 |
| 4.3.3.3.2. T2 | 30 |
| 4.3.4. OWR 85/15 | 30 |
| 4.3.4.1. Direct Weight Measurement | 30 |
| 4.3.4.2. UCA | 31 |
| 4.3.4.3. NMR | 32 |
| 4.3.4.3.1. 1D Profile | 32 |
| 4.3.4.3.2. T2 | 32 |
| 4.3.5. Summarized Results Of Direct Weight Measurement | 33 |
| 4.3.6. Geometric Mean T2 Relaxation Time | 33 |
| 4.4. Rheology | 34 |
| 5. Discussion | 35 |
| 5.1. OWR 70/30 | 35 |
| 5.2. OWR 75/25 | 35 |
| 5.3. OWR 80/20 | 36 |
| 5.4. OWR 85/15 | 36 |
| 5.5. T2 | 37 |
| 6. Conclusion | 38 |
| 7. References | 39 |
| Appendix A: Fig. A1-A25 | 41 |
| Appendix B: Formula for calculating geometric mean of the T2 relaxation time | 50 |
| Appendix C: NMR script for T2 and 1D profile experiments | 51 |

1. Introduction

Since the 23rd of December 1969 drilling for oil and gas outside the coast of Norway has been a profitable business. Numerous wells have been drilled, and new ones are still being drilled every year. The oil industry has become the most important contributor to the welfare of the Norwegian society. Over 40 years after the first oil was confirmed on the Norwegian continental shelf, new fields are still being discovered. There has been a need to search deeper and more remote areas to discover new oil, and new technology has been developed to be able to produce it in a profitable way. The North- Sea has been an arena for the oil and gas companies and many fields have been developed and produced. The activity is increasing in the Norwegian- Sea and the Barents- Sea. With the Alexander Kielland accident in the Ekofisk field in 1980 that claimed 123 lives it is well recognized that offshore operations off the coast of Norway is not without risk. The Deep Water Horizon incident in the Gulf of Mexico has reminded us that incidents not just strike human lives, but can also be catastrophic to the environment. Questions are asked if the industry is ready to take on the challenging environments in the north without taking too high risks for the environment and the people working on the installations.

Being able to operate within the margins of HSE specifications are of most importance in order to get access to new areas. Well control is one of the most important issues in order to do so. As the wells are drilled deeper, longer and more inclined, managing high pressures, high temperatures and wellbore instability is getting more demanding.

Since the late 1980s the sag phenomenon has been a serious subject of study in the oil industry (Omland 2004). Sag is the settling of weight particles that are suspended in a fluid, due to gravity. This can lead to operational problems, such as stuck pipe and problems running casing, and it can lead to serious accidents such as a blowout. The term "barite sag" is often used, because barite is usually used as weighting material in drilling mud (Zamora 2009). Ilmenite, hematite and manganese tetraoxide are also used to provide required density of drilling mud.

Since sag stability can be of the essence in order to maintain well control, research has led to development of a new mud system. The use of micronized weighting particles, with a tenfold reduction in particle size compared to the regular barite particles, gives a mud with minimum settling potential.

Being able to monitor sag in the field could lead to safer and more efficient operations. This study has been focusing on techniques to monitor sag, with a special attention on monitoring sag in micronized barite drilling fluids.

2. Theory

2.1. Barite sag

Barite is a dense mineral with specific gravity of typically 4.20 g/cm³. It comprises barium sulfate (BaSO₄), which is the most important weighting agent in drilling fluids (Mitchell 2011). Barite sag occurs in the wellbore when the suspended weight material in the drilling fluid starts to settle. This can lead to operational issues affecting both safety and economics. It may cause various technical problems such as well-control problems, stuck pipe, induced wellbore instability and lost circulation (Tehrani 2009). Sag is a more severe problem in synthetic- or oil-based drilling fluids than in water based drilling fluids (Omland 2004). Many factors are affecting sag in invert-emulsion drilling fluids. This includes operational parameters as well as fluid properties. Among the fluid properties affecting barite sag is rheology, density, solids content, particle size, particle size distribution, and interfacial chemistry of the dispersed solid and aqueous phases (Tehrani 2009). In 1996 Zamora et al. published a paper regarding the influence of drilling variables on barite sag. Tests were performed on a laboratory flow loop to evaluate key drilling parameters influence on barite sag. They found that angles of 60-75° and low annular velocities gave the highest sag. Drillpipe rotation may lower the barite settling, and even re distribute barite beds at the low side of the hole. By combining field observations with test results four areas of importance to minimize sag were addressed: well planning, mud properties and testing, operational practices, and wellsite monitoring procedures (Bern 1996).

2.2. Settling kinetics

2.2.1. Hindered settling

In Fig. 1 particles suspended in a fluid settle downward at a rate V_0 due to gravitation. In a vertical tube, there will be three regimes where the concentration of particles will increase from top to bottom with time until a state of equilibrium is reached. In the uppermost layer, the clarification regime, Stokes law will apply, see Eq. 1. The settling particles will have close to no influence on each other.

Below the clarification regime there will be what is called “hindered settling regime”. The rate of settling in this regime is slower than the rate of “free settling” in the clarification regime above. This is due to the higher concentration of particles, hence particles will interfere with one another. However, clusters of several particles may be formed that will settle faster due to the increased weight.

In the bottom of the tube particles accumulate and support each other mechanically. As the bed compacts due to the continuous accumulation of new particles, fluid is very slowly expelled upwards. This is called the “compaction regime” (Zamora 2009).

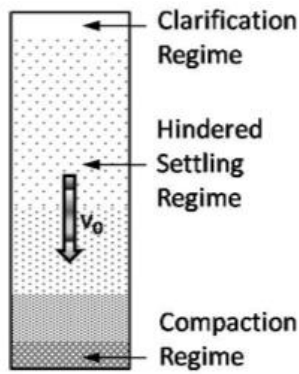


Figure 1: Particle settling in a vertical tube (Zamora 2009).

2.2.2. Boycott effect

Studies performed by Hanson et al. (1990) and Jefferson (1991), revealed that sag is higher in inclined wellbores than in vertical wellbores. This phenomenon was first discovered by the American physicist A.E. Boycott (1920). In 1920 Boycott noticed that blood corpuscles gravitate faster in inclined test tubes than in vertical test tubes. In an inclined tube, the vertical travel distance of the settling particles is reduced in comparison to a vertical tube. The particles settle vertically and sediment beds are formed on the low side of the tube. The sediment beds then slumps downwards and accumulates in the bottom of the tube. The clarified layer moves upwards to the high side of the tube. This is an accumulation of displaced fluid. Due to buoyancy, the clarified layer flows upwards and the thickness of the layer increases from the bottom to the top of the tube. This has an accelerating effect on particle settling since the displaced fluid can easily move out of the way (Zamora 2009).

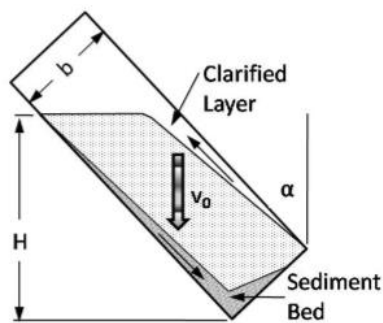


Figure 2: Particle settling in an inclined tube (Zamora 2009).

2.3. Stokes law

Stokes law describes how one single, spherical particle is settling in a fluid. It does not take into account particle- particle interaction or temperature effects. Stokes law is expressed by the equation:

$$V_T = \frac{2Rg(\rho - \rho_0)}{9\mu} \quad (1)$$

Where V_T is the settling velocity of the particle, R is the radius of the particle, ρ is the density of the particle, ρ_0 is the density of the suspending fluid and μ is the fluid viscosity (Omland 2007).

2.4. Rheological properties influence on sag

Several studies have been focusing on relating static and dynamic sag with rheological properties of the drilling mud. Among these are Saasen *et al.* (1991), Dye *et al.* (1999) and Tehrani *et al.* (2004). Due to its complexity, this will not be much covered in this work. However, by looking at Stokes law, one realize that increased fluid viscosity is decreasing the velocity of the settling particle. This is at least valid for one particle settling in a fluid. Even though it is not straight forward to predict the sag potential from rheology properties, gel formation seems to be important for avoiding static sag, while low shear rate viscosity is an important parameter affecting dynamic sag (Saasen 1996).

2.5. Micronized weight particles

The drilling industry have the recent years faced new challenges as a result of seeking deeper and more remote areas for undiscovered hydrocarbon resources. In some cases, in order to reach the target, there has been a need to drill long well- sections. This has brought up a challenge in balancing the well pressure in between a narrow pressure window above the pore pressure and below the fracture pressure. By the use of micronized weighting particles one is able to make a drilling mud that has a low viscosity, and due to the reduced size of the weight particles, a low sag potential. This reduces the ECD (Equivalent Circulating Density) and enables to balance the pressure in the well within the narrow operating pressure window.

The barite particles are treated with a specially developed technology. By milling the particles in an enhanced mineral oil, they get an effective oil wet surface. This makes it possible to produce a stable oil based slurry with high solids content, high density and low viscosity. The slurry is used as a base, and additives like emulsifier, fluid loss control and brine is added to make up a complete drilling fluid. One typical specification of the barite particles may be that 60% of the particles are less than 2 micron (Taugbøl 2005).

2.6. Sag determination techniques

Several methods have been proposed for sag detection in the oil industry. Some techniques are applicable as in-field measurements while others are to be used in the laboratory only due to quite complicated setups that require much space and strictly controlled testing environments, such as temperature control and pressure control. These test setups may be able to monitor several parameters related to the sag phenomena and contribute to a better understanding of the phenomena which again may lead to improved design of drilling and completion fluids. The in-field testing methods are quite simple and one of them is based on the well-known Fann Viscosimeter (Omland 2009).

2.6.1. Static sag testing

A common method for measuring static sag is to pour the fluid of subject into a steel cell and put the cell into an oven at a specified temperature and leave it to age statically for a required time. Typically testing temperatures are 90 degrees Celsius or 120 degrees Celsius. Then the clear fluid called the “free layer” on top is removed, and the fluid column in the cell is divided into five segments. The density of the top and bottom layer is measured using a pycnometer and a scale weight and the sag factor, SF, is found by the formula:

$$SF = \left(\frac{MW_{bottom}}{MW_{bottom} + MW_{top}} \right) \quad (2)$$

Where MW_{bottom} and MW_{top} are the densities measured at bottom and top of the cell respectively. A non-sagging fluid has a SF of 0.5, while a SF of 0.52 or higher can potentially indicate operational problems. Since the free liquid on top of the fluid is removed after aging, the SF does not take syneresis into account. This effect can be included by introducing a dynamic sedimentation index that compares the bottom mud weight with the initial mud weight (Omland 2004).

The method has not been accepted as an industry standard. It does not take into account operational conditions that are highly related to dynamic sag, it has proven difficult to implement, and the method is crude and has shown problems in reproducibility (Omland 2007). However, the test method seems to give more reproducible results when it is used on very stable mud samples for instance mud containing micronized particles.

2.6.2. Viscometer dynamic sag testing

In order to measure the dynamic settling regime the viscometer sag test (VST) was introduced. It has the advantage of simplicity, as it is built on a Fann 35 viscometer. The test setup is practical for use offshore and is also low-cost, considered it depends on equipment that is already available on the rig. The mud is put in a thermo cup and sheared for 30 minutes. Then the fluid density at the bottom of the thermo cup is measured and compared to the initial fluid density to give an indication of sag (Omland 2007).

The VST has been modified by placing a thermoplastic “shoe” at the bottom of the viscometer cup. The “shoe” has a sloping surface that adds another two advantages to the test method; it accelerates the settling process according to the boycott effect, and it collects the weight material at the bottom of the thermo cup. This contributes to increased sensitivity and reproducibility of the test method. The measure of sag is given by the “sag register”, S_R :

$$S_R = \left(-k \frac{\Delta MW}{MW} \right) \quad (3)$$

Where ΔMW is the measured difference in density of the drilling fluid at the bottom of the thermo cup between two runs, MW is the initial density, and k is a correlation constant equal to 10.9 for the modified VST. S_R values below 1.0 indicate sag while a S_R value of 1.0 equals no sag (Omland 2007).

2.6.3. Sag flow loop

The sag flow loop is a sophisticated sag detection setup that is used in laboratories at universities and by petroleum industry companies to better understand the physics behind sag and the parameters influencing the phenomena. The setup is too complex and requires too much space to be suitable for fluid optimization at the rig site. The flow loop is often used to establish a base line when new fluid systems are developed towards increased sag stability. It has also been used as a quality measure before applying any new fluid in the field (Omland 2007). Even though the flow loop is able to measure dynamic sag under different conditions, it has not yet the ability to really simulate down-hole environment. What happens down hole during an operation is very complex and to simulate it means

to reproduce hole geometries, temperature effects, mechanical influence of the drill string etc., which in reality may seem like an impossible task.

2.6.4. High Angle Sag Test Device

The HAST (High Angle Sag Test Device) can take into account parameters like pressure, temperature and hole angle effects to simulate down hole conditions. The setup is accurate and do not demand as much space as the sag flow loop (Jamison 2003). In the HAST the fluid is placed in a tube. The temperature, pressure and the angle of the tube is specified for the certain test. The center of mass will gradually shift and this is measured as the change of torque on the tube in the oblique position. The change in center of mass as the weighting material is settling is plotted as a function of time using:

$$X_{cm} = \left(\frac{At}{B+t}\right) \quad (4)$$

Where A is the maximum shift in center of mass. B is the time when half of the material have settled. The sag coefficient, SC , is given by integrating the function of time and is indicating the total sag that has occurred as given by:

$$SC = \int_{t=0}^t X_{cm}(t)dt \quad (5)$$

If there is no sag, SC is zero, which means that there has been no movement in the center of mass (Omland 2007).

2.6.5. Direct weight measurement

Direct weight measurement is a testing technique that directly monitors the settling rate of the weight particles in the fluid by the use of a laboratory scale that measures the weight of the particles that falls out of suspension. This is done by pouring fluid into a cylinder with a collecting cup in the lower end that collects the weight particles. The collecting cup is connected to a laboratory scale by a steel rod allowing for continuous monitoring of the weight of the collected weighting material. By the use of a modified atmospheric consistometer it is possible to rotate an outer cylinder that simulates the rotation of a drillstring. It is also possible to set the temperature of the test with a water bath (Omland 2010).

2.6.6. Ultrasonic measurements for sag detection

Ultrasonic measurements have been used (Bamberger 2004) to identify density stratification in fluids by measuring the speed of sound travelling through the media, as the speed of sound is affected by changes in density. As the signal reflection for ultrasound is also dependent on the longitudinal speed of sound in the material reflecting the signal, reflecting particles shape, size and concentration, ultrasonic measurements may have the potential for sag analysis in the drilling industry. Ultrasonic measurements also have the advantage of continuous, non-invasive monitoring of the drilling fluid. However, one might run into difficulties when applying this technique on fluids with high solids concentration (Omland 2007). Investigations done by Egeland (2009) has also suggested that ultrasonic sound waves have an impact on the settling rate of weighting materials.

2.6.7. Sag detection using NMR

Nuclear Magnetic Resonance (NMR) measurements makes it possible to determine the hydrogen content and distribution in a fluid placed in a test tube. This is done by detection of the nuclei spin of the hydrogen atoms in the fluid caused by absorption of electromagnetic radio waves from a strong magnetic field (Omland 2007). By analyzing the strength of the reflected signal one is able to determine the concentration of suspended particles in the fluid. Since particles falling out of the suspension expel the liquid phase, the signal will be increasing upward in the sample as the measurements progress in time if sag is present. As solid particles do not reflect any signal, any accumulation of solids at the bottom of the test tube is indicated by weak signal strength. This is shown by work performed by Rismanto and Van der Zwaag (Rismanto 2007), and the conclusion of their work indicated that the application of NMR might have a huge potential in analyzing sag using 1D profiling. The NMR sag detection method is non-invasive and unlike the ultrasonic measurement, it is not restricted by the solids concentration in the fluid.

By performing measurements on longitudinal relaxation time T1, and transverse relaxation time T2, Rismanto and Van der Swag also found correlation between T1 and T2 and varying oil-water content in drilling fluids, indicating yet another possible application area of NMR (Rismanto 2007).

2.6.7.1. NMR measurement principle

Hydrogen has a net magnetic moment or spin. A measurable signal is produced when an atomic nuclei, in this case the hydrogen atom, interacts with a superimposed magnetic field (Coates 1999). The external magnetic field force the magnetic moment to precess around the field axis. The angular frequency of the precessional magnetic moment about the field axis is called the Larmor frequency (Lambert 2004).

The energy state of a proton subjected to an external magnetic field relies on the direction of the magnetic field and the orientation of the precessional axis of the proton. The longitudinal direction is the direction of the magnetic field. The high energy state of the proton is when the precessional axis is anti-parallel to the longitudinal direction. The low energy state is when the precessional axis is parallel to the longitudinal direction. The signal measured by the NMR instrument is the bulk magnetization, which is the difference in protons parallel and anti-parallel to the magnetic field (Coates 1999).

When a proton is subjected to a static magnetic field, the magnetic moment can be tilted by applying an additional oscillating magnetic field with an angular frequency equal to the Larmor frequency (Coates 1999). By applying a magnetic field that is oscillating at either 90° or 180° pulse frequency, the magnetic moment is aligned in the transverse or longitudinal direction, respectively. When the oscillating magnetic field is turned off, the precession of the protons will tip back, and the bulk magnetization will decrease due to that the precession of the protons will no longer be in the same phase. The longitudinal relaxation time, T1, is the length of the decaying signal to align with the longitudinal direction. The transverse relaxation time, T2, is the length of the decaying signal to align with the transverse direction (Coates 1999, Lambert 2004).

2.6.7.2. Relaxation mechanisms

There are three types of relaxation mechanisms, which will affect the relaxation time of the proton spin. That is bulk relaxation, surface relaxation and diffusivity relaxation.

The bulk relaxation is the characteristic relaxation time for one pure bulk fluid. It is depending upon physical properties, such as viscosity, and properties of the environment, such as pressure and temperature.

The surface relaxation causes an additional relaxation mechanism to the bulk relaxation time, and make the fluid relax faster at the surface of the grain than in the bulk phase. The surface relaxation make the NMR sensitive to wettability, because the fluid (oil or water) that is in direct contact with the surface of the grain has a shorter relaxation time than the bulk value. The fluids that are not in contact with any grains react as bulk fluid.

The third relaxation mechanism is relaxation due to diffusion. In a magnetic field gradient the T2 relaxation is enhanced by molecular diffusion (Cheng 2005).

3. Experimental Work

Initial tests were performed on a simple water based mud referred to as UIS WBM, and a simple oil based mud. This mud was referred to as UIS OBM. Composition and mixing procedures can be found in Ch. 3 for both fluids. These tests were carried out in accordance with testing procedures described by Mjøllhus (2011). The purpose of running these tests were to calibrate testing procedures, including the preparation of the mud and the testing equipment in order to get reliable results when applying these methods on a new type of mud where the results were yet unknown. The initial tests comprises direct weight measurement using a modified consistometer, and registration of transition time of ultrasonic sound waves using an ultrasonic cement analyser (UCA). The results from these tests are presented under section 4.1 and 4.2 in Ch. 4.

After establishing proper routines in the laboratory by performing testing on UIS mud and comparing the results with previous work performed using the same fluids and equipment, the experimental investigations were carried out on oil based mud containing micronized weighting particles. This mud is referred to as Halliburton OBM. Composition and mixing procedures of the mud is described in Ch. 3. The mud was prepared with four different oil water ratios (OWR): 70/30, 75/25, 80/20 and 85/15. The amount of barite was kept constant in all different OWR. The Halliburton OBM is known to have a low sag potential and the mud was used in order to investigate whether the UCA and NMR measurement techniques are able to measure and identify sag in this low sag potential drilling fluid. The results from the UCA and NMR studies are analyzed and compared to the results from direct weight measurements, which in this case proves as the true sag detection. Due to a time limitation within this study, each individual test run was limited to 25 hours. The previous study on UIS mud performed by Mjøllhus (2011) indicated the need for a strict control of pressure, temperature and air bubble effect on the UCA measurements. The suggestion from this work was to vacuum the fluid sample for 5 min. prior to running the test, in order to release dissolved gas in the mud caused by the mud mixer, and to apply a pressure of 5 bars in order to keep the pressure constant during the test. Alternatively, to apply a pressure of 30 bars without vacuuming the fluid sample. The first suggestion have been applied in this study. In order to be able to compare the results from the different tests, the mud were treated in the same way prior to both UCA, NMR and direct weight measurement. The test temperature was set to 35°C since this is the working temperature for the NMR instrument.

3.1. Mixing procedures

3.1.1.1. WBM

The fluid was prepared by the use of a Hamilton Beach mixer.

1. Start by weighting up the amount of water in the mixing cup.
2. Weight up drispack, and add carefully in the mixing cup at low speed.
3. Mix at high speed for 2 min.
4. Weigh up the amount of barite and add to the mixing cup.
5. Mix at high speed for 3 min.

3.1.1.2. OBM

The fluid was prepared by the use of a Silverson L4RT-A laboratory mixer with an impeller screen with squared holes to obtain proper shear when mixing. The mixing speed was set to 6000 rpm. The mixing cup was placed in a cooling bath to keep the temperature in the drilling fluid below 62°C in order to prevent the fluid agents from degenerating.

1. Place the mixing cup on a laboratory scale and weigh up the correct amount of mineral oil.
2. Weigh up CaCl₂ brine, emulsifiers (PE & SE) and lime and add to the mixing cup.
3. Mix for 8 min.
4. Weigh up viscosifier (Versavert Vis) and add to the mixing cup.
5. Mix for 8 min.
6. Weigh up fluid loss additive (Versatrol) and add to the mixing cup.
7. Mix for 4 min.
8. Weigh up the weighting material (barite) and add to the mixing cup.
9. Mix for 10 min.

3.1.2. Halliburton OBM

The fluid was mixed at 6000 rpm (\pm 300 rpm) over a total of 60 minutes. Four lab barrels which equals 1.4 liters (one lab barrel equals 350 ml) was prepared at one time. The mixing was done by use of the Silverson mixer described earlier. Close attention was kept at the temperature during mixing as for the UIS OBM.

1. Place the mixing cup on a balance and weigh out the amount of base oil.
2. Add primary and secondary emulsifiers. Mix for 5 minutes.
3. Add fluid loss control agents. Mix for 5 minutes.
4. Add Viscosifier. Mix for 10 minutes.
5. Add lime. Mix for 5 minutes.
6. Place the mixing cup in a water bath. The fluid temperature should be between 50-55 degrees Celsius in order to obtain the correct yield. The fluid temperature should not rise above 62 degrees Celsius as this may degenerate the fluid agents.
7. Continue mixing while brine is added. Verify that the mixing is good. Mix for 15 minutes.
8. Add weighting agent. Mix for 15 minutes.

3.2. Mud Composition

3.2.1. UIS WBM

Table 1: *Composition of UIS WBM.*

| Product | Function | Amount |
|----------------------------|-----------------|---------|
| Water | Base fluid | 350 ml |
| Polypac regular (drispack) | Viscosifier | 2 g |
| Barite | Weight material | 138.8 g |

3.2.2. UIS OBM

Table 2: *Composition of UIS OBM.*

| Product | Function | Amount |
|--------------------------|---------------------|--------|
| EDC 95/11 | Base fluid | 206 ml |
| CaCl ₂ brine* | Salt | 60 ml |
| PE | Emulsifier | 3 ml |
| SE | Emulsifier | 9 ml |
| Lime | Alkalinity | 8.5 g |
| Versavert Vis | Viscosifier | 5.5 g |
| Versatrol | Fluid loss additive | 6 g |
| Barite | Weight material | 150 g |

*Premade brine: SG=1.162

3.2.3. Halliburton OBM

Table 3: *Composition of Halliburton OBM. Oil and brine content is varied for different OWR. See table 4.*

| Product | Function | Amount |
|--------------------------|-----------------|-----------|
| EDC 99 DW | Base fluid | X ml |
| Perfor Mul | Emulsifier | 56 g |
| Drilltreat | Wetting Agent | 7 g |
| Geltone II | Viscosifier | 14 g |
| Adapta | Filtration | 5.6 g |
| Lime | Alkalinity | 28 g |
| CaCl ₂ brine* | Salt | X ml |
| Bariflor 8004 | Weight material | 1423.65 g |

*Premade brine: SG=1.19

Table 4: Oil and brine content in Halliburton OBM.

| OWR* | Base fluid | Brine |
|-------|------------|-----------|
| 70/30 | 685.02 ml | 293.58 ml |
| 75/25 | 705.6 ml | 273 ml |
| 80/20 | 782.88 ml | 195.72 ml |
| 85/15 | 831.81 ml | 146.79 ml |

*The concentration of different fluid agents have been kept constant, which means that the OWR is not exact values. The given OWR values are only based on content of base fluid and brine, which gives an approximated OWR value.

3.3. Test Equipment

3.3.1. Direct Weight Measurement

The direct weight measurement test setup consist of a modified atmospheric consistometer coupled to a laboratory scale as shown in Fig. 3. An external water bath has also been added to the setup in order to keep the test temperature stable. The consistometer is normally used to determine the thickening time of cement slurries and for preparation of cement slurries before rheological measurements. The benefit of modifying a consistometer for the purpose of performing direct weight measurements is the ability to rotate the outer cylinder to simulate drill string rotation during testing. A sampling cup is placed near the bottom of the outer cylinder. As the suspended weight particles settle, they accumulate in the sampling cup. A steel rod connects the sampling cup to a laboratory scale that is aligned with the sampling cup, so that the sampling cup can hang freely inside the outer cylinder. An inner cylinder is placed above the sampling cup to provide a settling chamber. There is a maximum amount of settling possible before the particles start to build up below the sampling cup so that this will affect the weight readings. Change of density in the test fluid due to settling may also affect the weight readings due to reduced buoyancy.



Figure 3: Direct weight measurement setup consisting of a modified atmospheric consistometer connected to a laboratory scale by a steel rod.

3.3.2. UCA

The test setup for the UCA measurement technique consists of an Ultrasonic Cement Analyser (UCA), model UCA 220V-50Hz seen in Fig. 4, air pressure supply (5 bars), a water bath, and a logging program titled Chandler 5270 Data Acquisition and Control System (DACS) Version 2.0.152 which registers temperature [°C] and transit time [$\mu\text{s}/\text{in}$].

The test cell is filled with the drilling fluid and placed in the apparatus. The air pressure supply, the thermometer and the sending transducer is connected on top of the cell. The receiving transducer is located in the apparatus and connected to the bottom of the cell when the cell is placed in the apparatus. The sending transducer at the top of the cell emits pulsating ultrasonic sound with a frequency of 400 kHz. The sound wave travel through the test fluid and the receiving transducer registers the waves at the bottom of the cell. The computer calculates the transit time [V^{-1}] in the fluid based on the registered signal and the known distance between the sending- and receiving-transducers.



Figure 4: UCA and steel test cell with temperature control, pressure supply and signal transducer connected.

3.3.3. NMR

A Maran Ultra bench-top NMR spectrometer from Oxford Instruments as shown in Fig. 5 was used for the NMR measurements. The instrument has an operating permanent magnet. The proton resonance frequency is 2 MHz. The test temperature of the NMR instrument is 35°C.



Figure 5: NMR instrument and test tube filled with Halliburton OBM.

3.4. Test Procedures

The fluids were vacuumed in a vacuum chamber for 5 min. and heated to 35°C prior to running the tests. For the modified consistometer, the testing equipment was preheated to 35°C before the fluid was poured into the test cup. The same was applied for the UCA, -here the test cell was preheated to 35°C before it was filled with the test fluid.

When running the UCA measurements, a constant pressure of 5 bars was applied during testing in order to manage the air bubble effect caused by gas in the liquid.

4. Results

4.1. UIS WBM

4.1.1. Direct weight measurement

Fig. 6 shows the weight of settled particles for UIS WBM, measured in grams, as a function of time. The test temperature was 20°C. After 5 hours over 50 grams of weighting particles had already settled, and during the next 15 hours about 15 grams of barite settled.

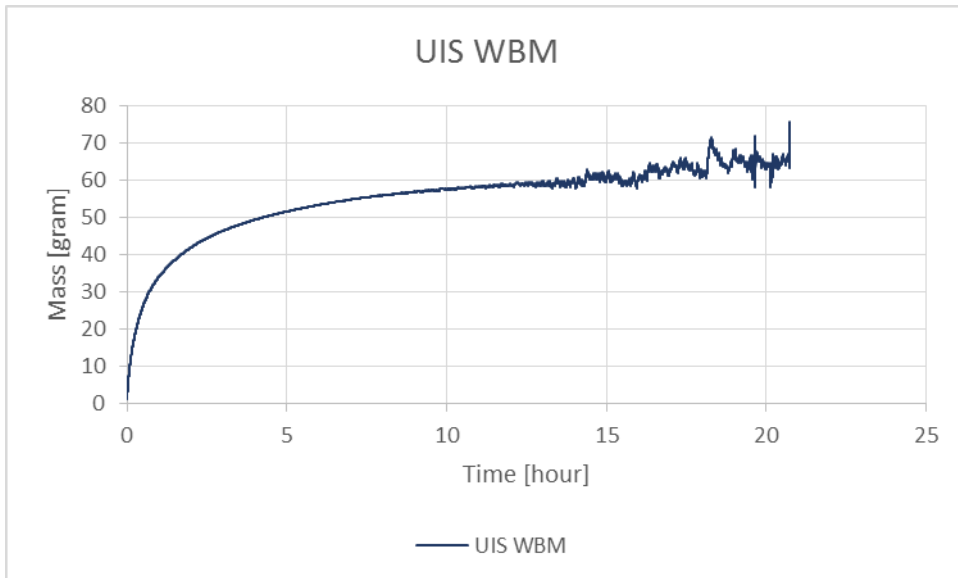


Figure 6: Recorded weight for settled weighting material as a function of time for UIS WBM.

4.1.2. UCA

Fig. 7 shows the result from an UCA test performed on UIS WBM. The upper (red) curve shows the temperature. The temperature scale is set to the secondary Y-axis. The lower (blue) curve is the recorded transit time, measured in microsec/in. The X-axis is time in hours. The transit time decreases rapidly the first minutes of the test before the trend turns and an increasing trend is seen for the transit time. After 15 hours the transit time stabilizes at 17.395 microsec/in. The test temperature was 20°C.

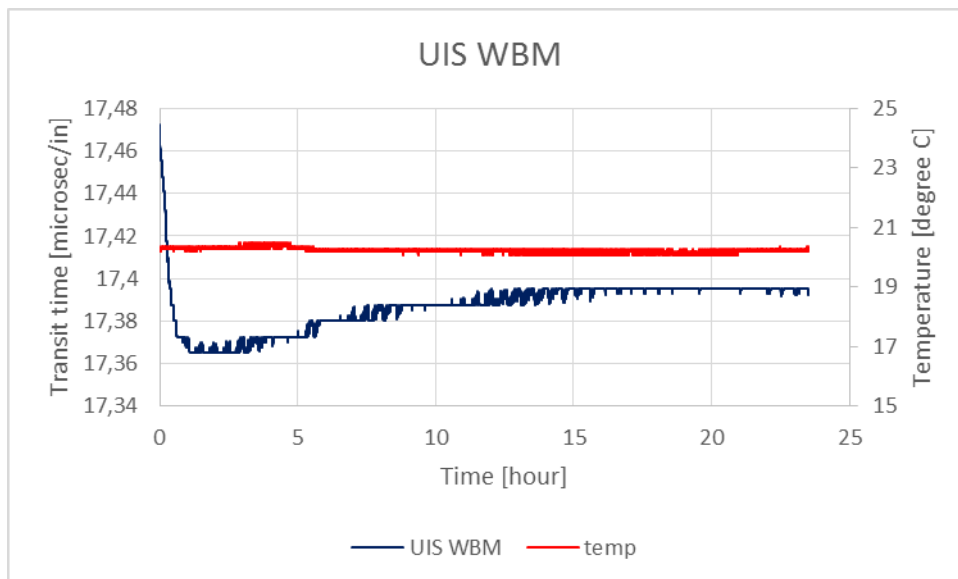


Figure 7: *Transit time and test temperature as a function of time.*

4.2. UIS OBM

Several attempts were done to test the UIS OBM on the UCA. Initial tests were done with the mud described in Ch. 3 at a test temperature of 20°C. The UCA was not able to read any signal. The amount of barite was varied from 0 g to 350 g, and tests were performed with temperatures of 20°C, 35°C and 50°C. Pressures of 5 bars, 30 bars and 200 bars were applied. The vacuuming time was varied from 1 min. to 5 min. There were also tests performed where the fluid was degassed by the use of sonification instead of a vacuuming chamber. The amount of viscosifier was also varied. A signal was registered by the UCA one time, at a test temperature of 35°C, and with an applied pressure of 5 bars. The fluid was vacuumed for 5 min. before the test. After a few hours the signal was lost.

4.3. Halliburton OBM

4.3.1. OWR 70/30

4.3.1.1. Direct weight measurement

Fig. 8 displays the result from direct weight measurement on Halliburton OBM with OWR 70/30. The curve shows the registered weight of the particles that have settled as a function of time. The weight is given in grams on the Y-axis, and the time on the X-axis is presented in hours. The rate of settling was highest in the beginning, and decreased smoothly and continuously throughout the test period. At the end of the test, particles were still settling, but the curve had started to flatten out. After 20 hours 3.38 grams had settled as repeated in Table 5. The test temperature was 35°C.

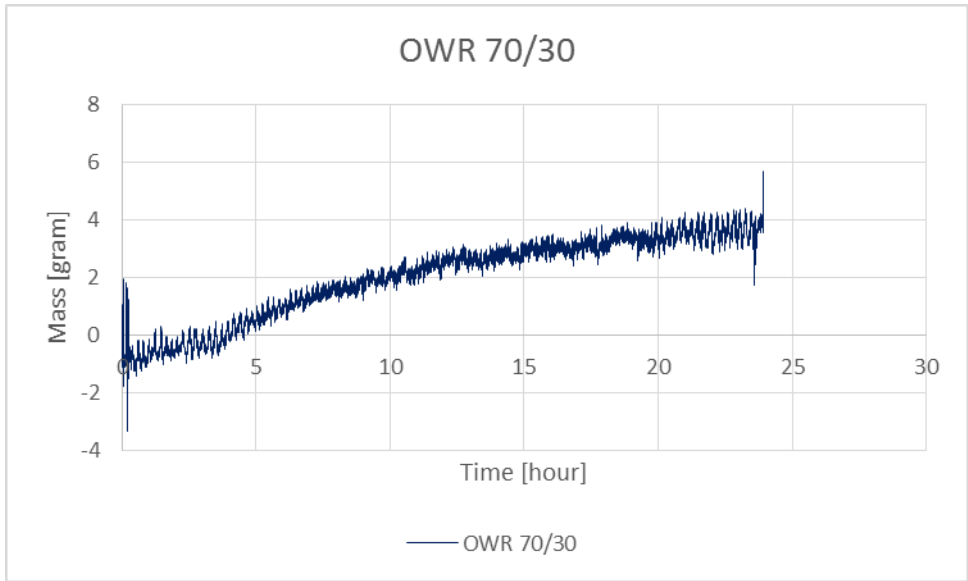


Figure 8: Recorded weight of settling weighting material plotted versus time for Halliburton OBM with OWR 70/30.

4.3.1.2. UCA

Fig. 9 displays the results from the UCA measurements on Halliburton OBM with OWR 70/30. The upper (red) curve is the recorded test temperature, and the lower (blue) curve is the recorded transit time, both plotted versus time. The transit time is given in microsec/in, the temperature is given in degree Celsius, and the time is given in hours. The transit time has a steep decrease for the first minutes of the test before it slowly increases over the next hours. From five hours until ten hours of the test period the transit time is stable. After ten hours one can see a decrease in the transit time before it stabilizes at a lower value until the end of the test. The test temperature was kept constant at 35°C.

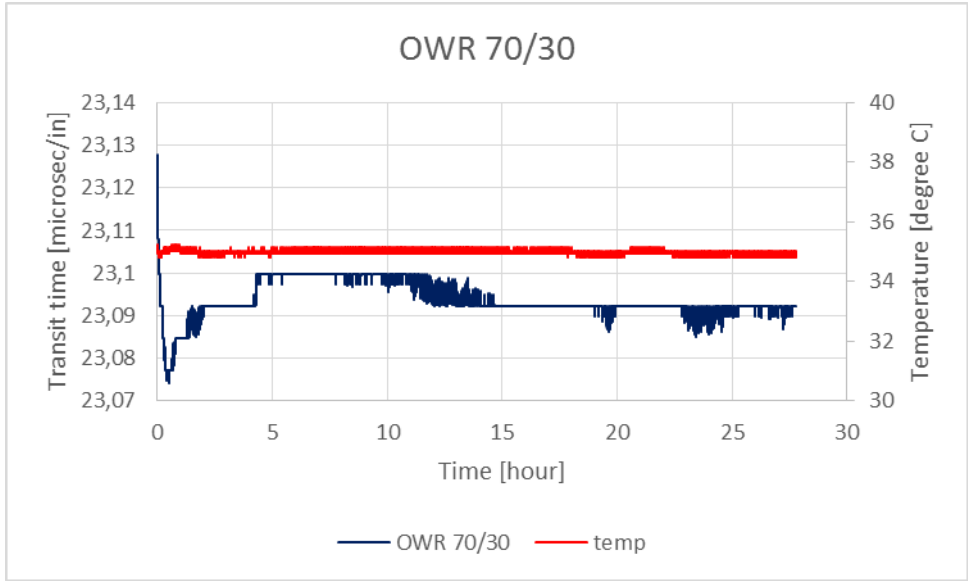


Figure 9: Transit time and temperature as a function of time.

4.3.1.3. NMR

4.3.1.3.1. 1D Profile

A 1D profile of Halliburton OBM with OWR 70/30 is shown in Fig. 10. On the Y-axis, 0 cm refers to the bottom of the test tube. 6 cm refers to the top of the fluid sample. The X-axis represents NMR signal amplitude. The continuous (blue) line is the 1D profile taken at the beginning of the the first hour of the test. The dotted (red) line is the measurement performed after 24 hours. The difference between the two profiles is small. There seems to be a small gap between the curves at the bottom of the sample, where the profile after 24 hours has a smaller amplitude. In general it looks like the amplitude is larger towards the bottom of the tube.

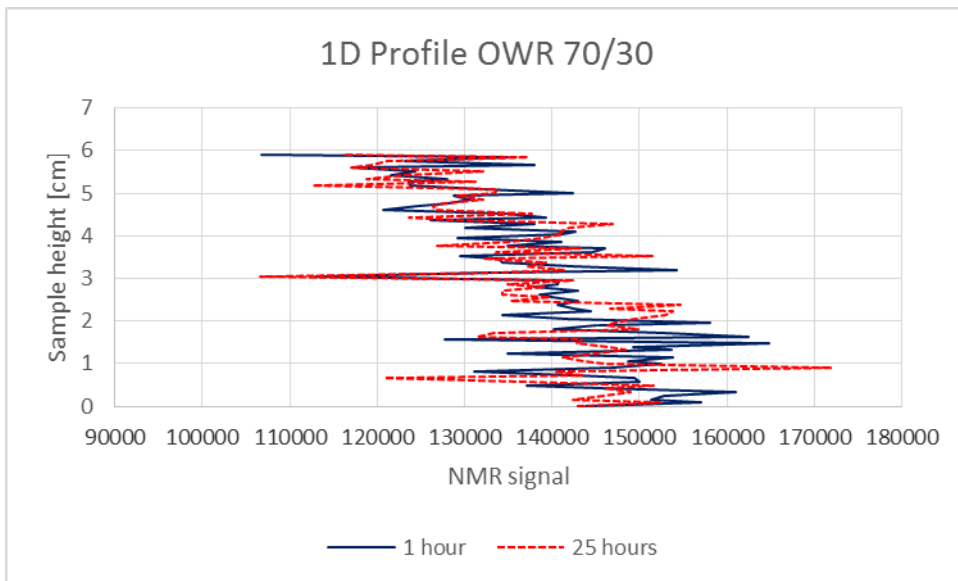


Figure 10: 1D profile for Halliburton OBM sample with OWR 70/30.

4.3.1.3.2. T2

Fig. 11 shows the T2 relaxation time measurement for Halliburton OBM with OWR 70/30. The curve represents the registered NMR signal as a function of time. The NMR signal is normalized. The X-axis is time in milliseconds, and the plot is semi logarithmic. The peaks on the graph represent the highest NMR signal amplitude and correspond to the relaxation time for the protons spin in the most common state in the fluid. The biggest peak probably shows the bulk relaxation time for the fluid, which is the relaxation time for hydrogen nuclei bonded with oxygen into OH⁻. The main peak is quite narrow, indicating a high degree of homogeneity in the fluid.

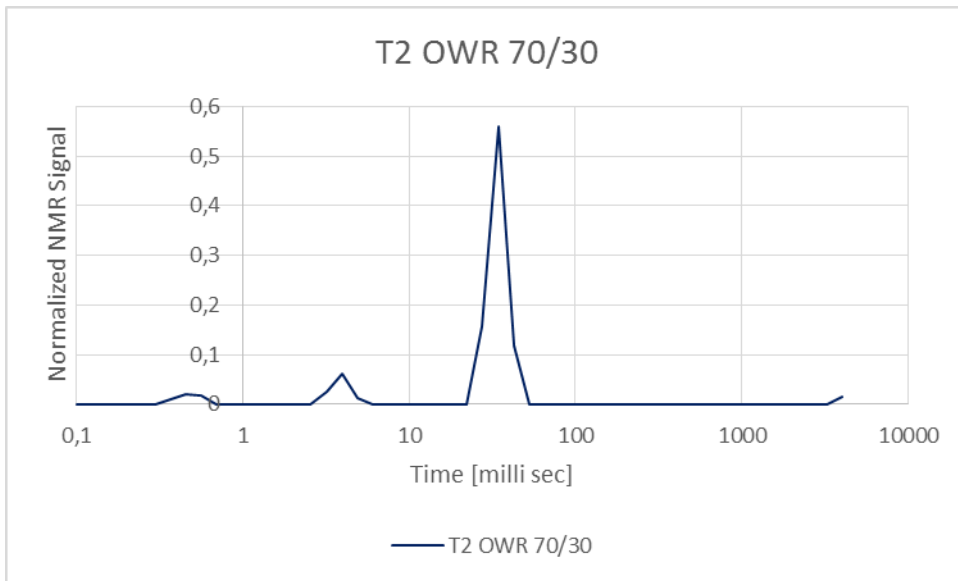


Figure 11: *T2* relaxation time for Halliburton OBM with OWR 70/30.

4.3.2. OWR 75/25

4.3.2.1. Direct weight measurement

Fig. 12 represents direct weight measurement of Halliburton OBM with OWR 75/25. The Y-axis is as described earlier registered weight in the sampling cup measured in grams. The X-axis represents time in hours. The settling is almost constant for the first 20 hours, when the rate of settling starts to decrease. After 20 hours the amount of settled material is 3.27 g which is almost the same as for the fluid with OWR 70/30. The test temperature was the same as for the mud with OWR 70/30, 35°C.

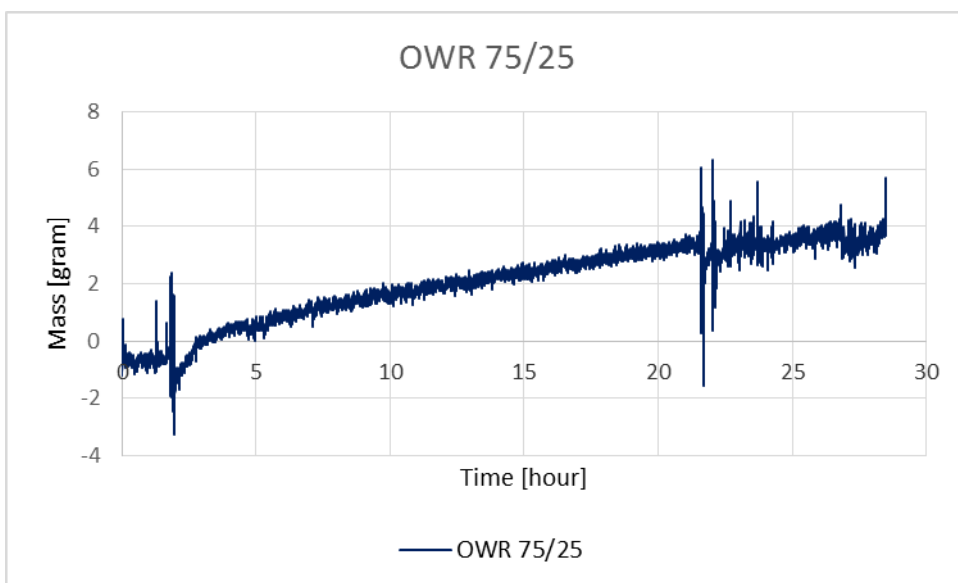


Figure 12: *Weight of settled weighting material as a function of time.*

4.3.2.2. UCA

Fig. 13 presents the results from the UCA test on Halliburton OBM with OWR 75/25. One can see that the temperature have been constant, but slightly below 35°C. The trend seem to be the same as in the test performed on the test fluid with OWR 70/30. A steep decrease in transit time is seen during the first minutes of the test before the transit time increases for a few hours after which begin to decrease again. At the end of the test the transit time once again started to increase after a period of 15 hours where decreasing trend was observed.

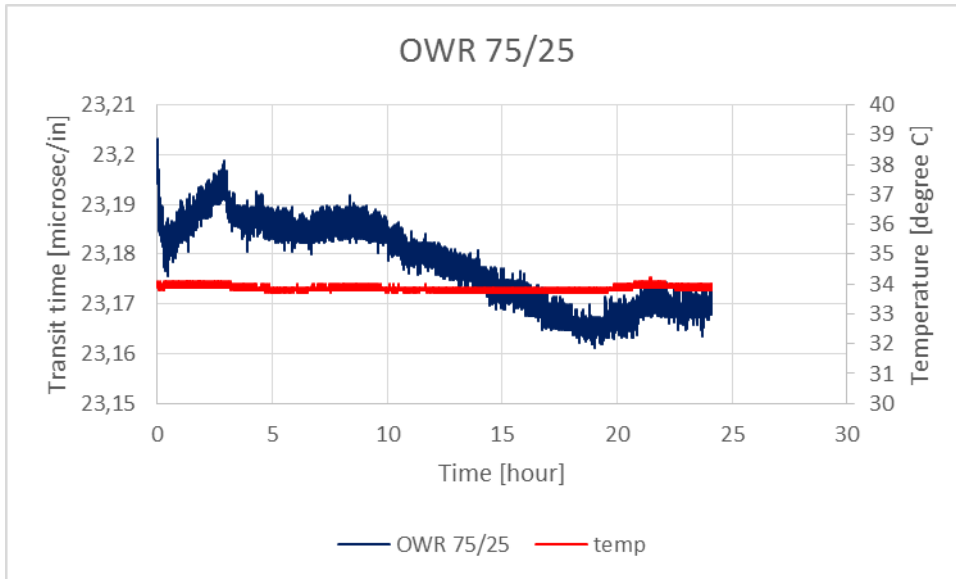


Figure 13: *Transit time as a function of time plotted together with test temperature.*

4.3.2.3. NMR

4.3.2.3.1. 1D Profile

A 1D profile for Halliburton OBM with OWR 75/25 is displayed in Fig. 14. The Y-axis is, as described for the 1D profile on OWR 70/30, corresponding to the height of the fluid sample. The X-axis represents the NMR signal amplitude values. There is not much difference in the NMR signal amplitude for the two measurements. The signal amplitudes seem to be increasing towards the bottom of the sample. Three cm above the bottom of the sample there was registered a peak at both the first and the last measurement. At the bottom of the sample the test results shows an increase in signal strength after 24 hours. That is the opposite of what would be expected in relation to sag.

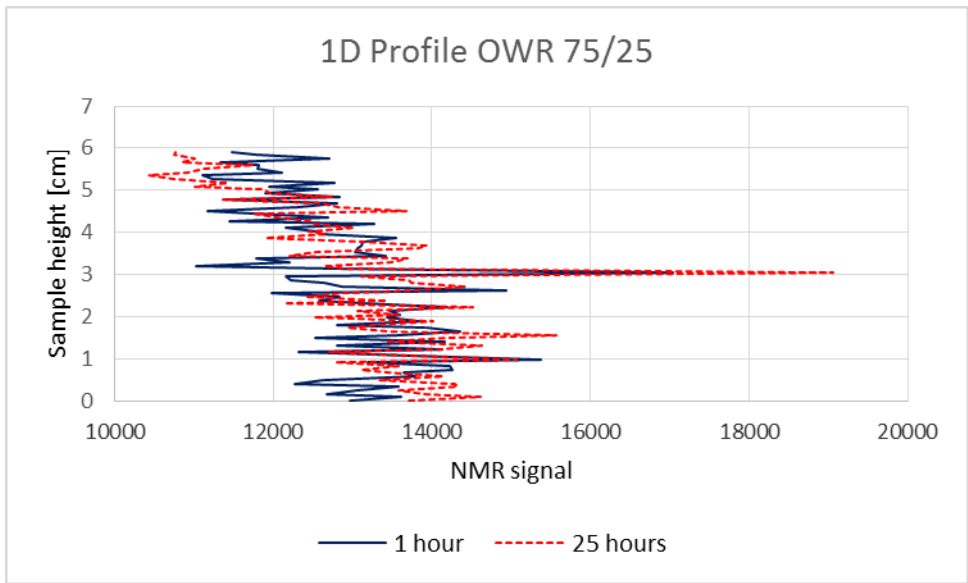


Figure 14: 1D profile of fluid sample with OWR 75/25.

4.3.2.3.2. T2

Normalized NMR signal is plotted as function of relaxation time in Fig. 15. The test fluid is Halliburton OMB with OWR 75/25. The time on the X-axis is given in milli seconds on a logarithmic scale. The relaxation time for the biggest peak has a wider distribution compared to the mud with OWR 70/30. As a result, the amplitude of the signal is lower, as the area under the graph represent the size of the decaying echoes directly related to the relaxation time T2.

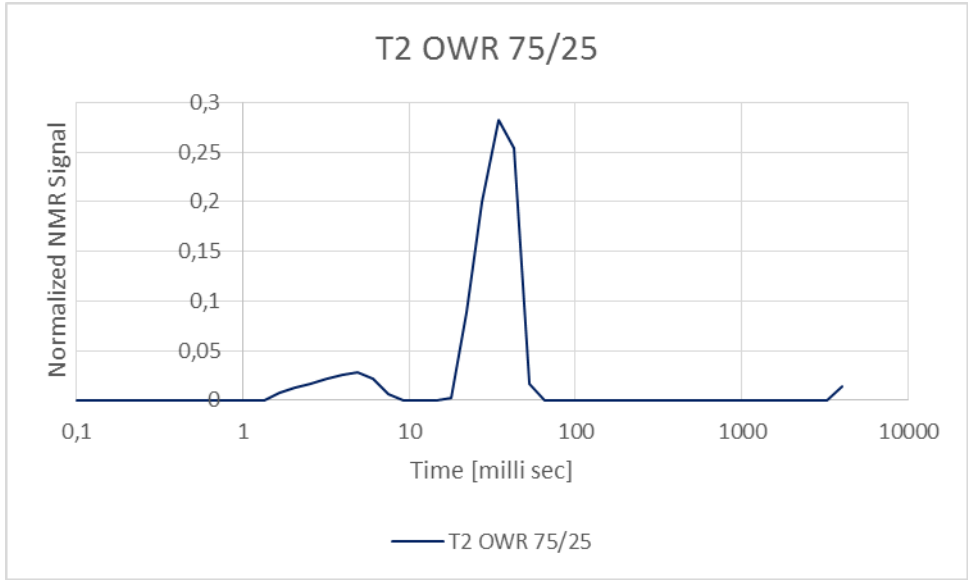


Figure 15: T2 relaxation time measurement for Halliburton OBM with OWR 75/25.

4.3.3. OWR 80/20

4.3.3.1. Direct weight measurement

The graph in Fig. 16 represents a direct weight measurement test. The test fluid was Halliburton OBM with OWR 80/20. The test temperature was as before, 35° C. The figure shows that there is a continuous settling of particles throughout the test period. The settling rate is highest in the beginning and lowest towards the end. The total weight of settled particles was about 5 grams at the end of the test. At time equals 20 hours, the registered weight was 4.89 grams, meaning that there was an increase of 1.62 grams from the test performed on the mud with 5% less oil.

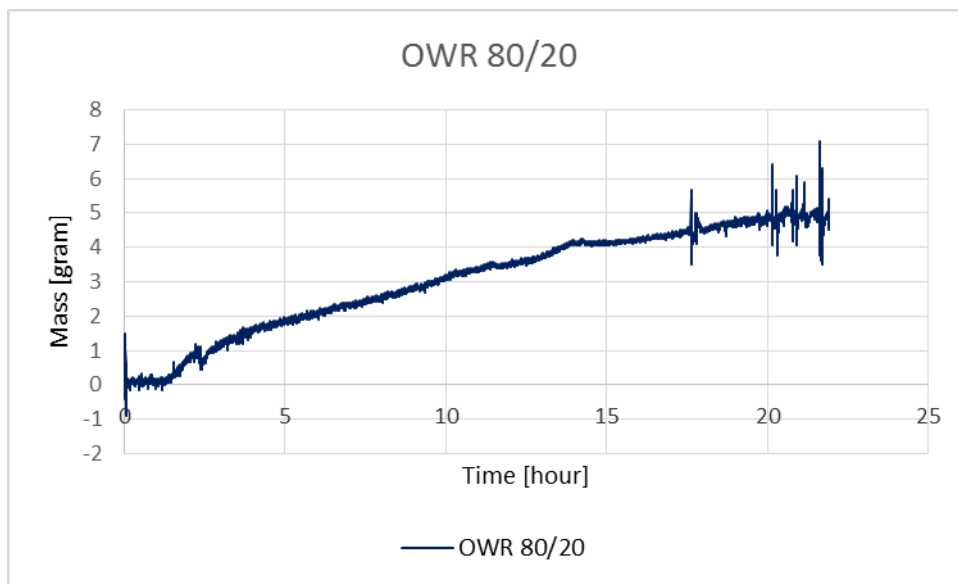


Figure 16: Direct weight measurement test on Halliburton OBM with OWR 80/20.

4.3.3.2. UCA

Fig. 17 is the result from an UCA test performed on Halliburton OBM. The OWR of the fluid sample is 80/20. The transit time in the test fluid goes through four cycles during the period of the test; a steep decrease is seen at first, followed by an increase, then the transit time decreases before it stabilizes for 5 hours, and in the end the transit time increases. The same thing has been seen with lower OWR, but the length of the cycles are different. In Fig. 17, the increase at the end starts 10 hours after the test was initiated, and continues throughout the test period.

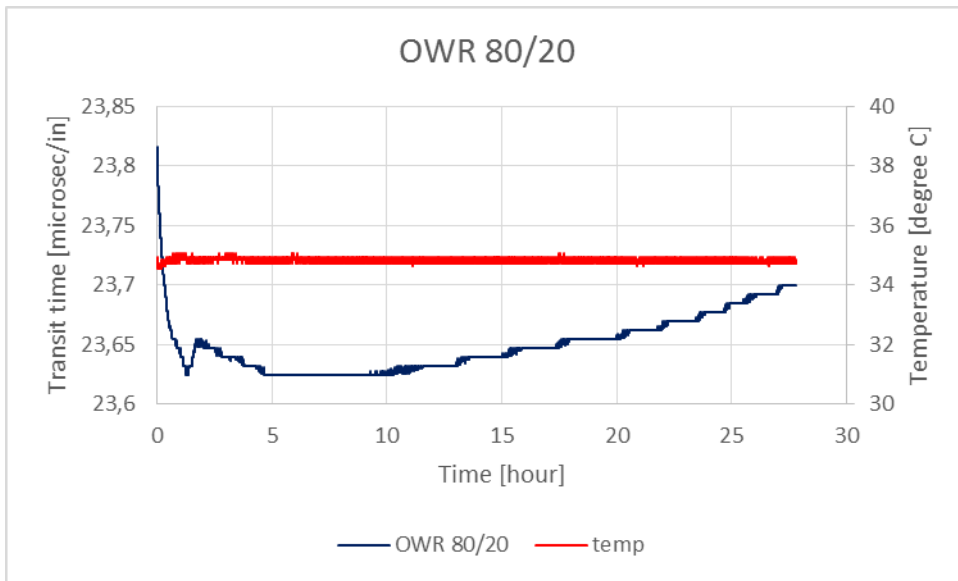


Figure 17: The graph shows the UCA test performed on Halliburton OBM with OWR 80/20.

4.3.3.3. NMR

4.3.3.3.1. 1D Profile

Fig. 18 shows NMR signal amplitude as a function of the height in the sample. As described earlier for the 1D profile experiments, the Y-axis represents the height of the fluid sample, where 0 cm is the bottom of the sample. The height of the fluid column was approximately 6 cm. Again, the continuous (blue) line represents the 1D profile for the beginning of the first hour, and the dotted (red) line is the result after 24 hours. After 24 hours a peak was seen in the NMR signal at the top of the fluid sample. Other than that the difference in the results of measurement performed at the beginning of the first hour and after 24 hours is small. The signal shows slightly increasing trend towards the bottom of the sample, as observed for previous samples.

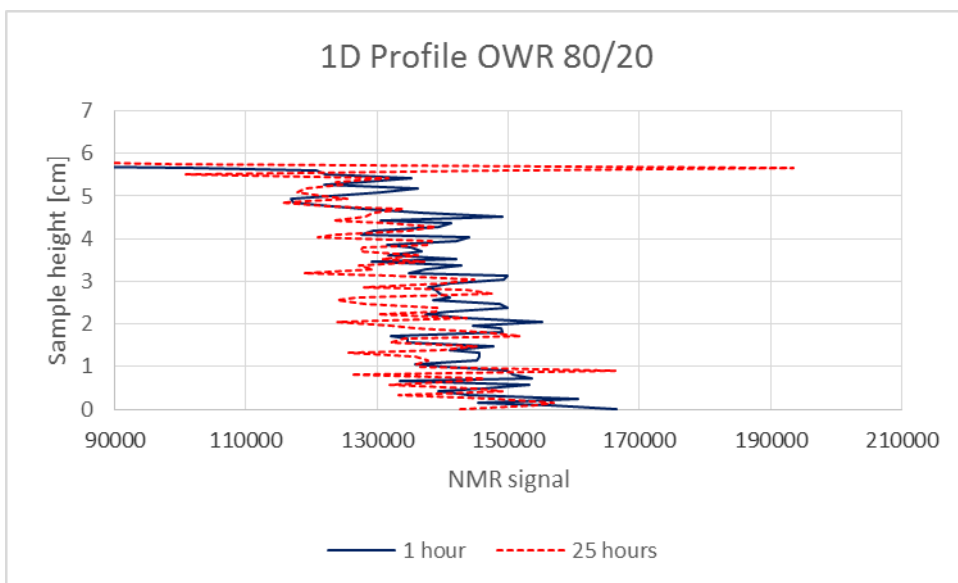


Figure 18: 1D profile of Halliburton OBM with OWR 80/20.

4.3.3.3.2. T2

The T2 relaxation time for Halliburton OBM with OWR 80/20 is plotted in Fig. 19. The relaxation time distributed under the main peak in the figure, is probably due to the bulk relaxation time of the fluid, but the result may also include contributions from surface relaxation and diffusivity relaxation. Compared to the T2 results presented before, the relaxation time distribution seems to grow with increasing OWR. This might be due to inhomogeneity in the magnetic field which again affects the relaxation time due to dephasing of the proton spin. This could be related to emulsion stability problems. That assumption is strengthened through the revealing of syneresis detected by the 1D profiling experiment for the same OWR.

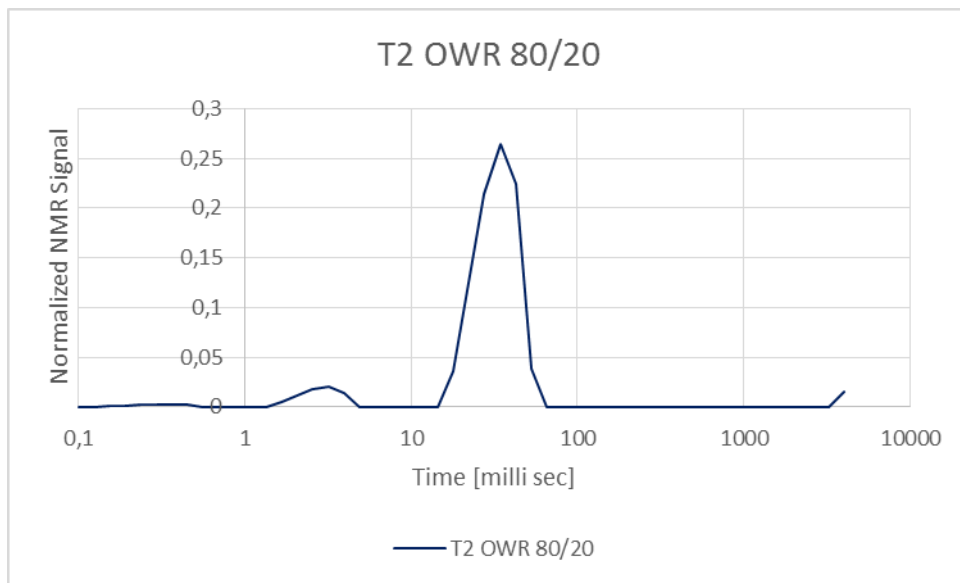


Figure 19: *Semi logarithmic plot of Normalized NMR signal amplitude as a function of T2 relaxation time.*

4.3.4. OWR 85/15

4.3.4.1. Direct weight measurement

The graph in Fig. 20 shows the direct weight measurement test of the Halliburton OBM with OWR 85/15. The settling takes place during the whole test period. The settling speeds up after the first two hours and is almost constant for the next 13 hours. After passing 15 hours in the test the settling rate starts to decrease. At the end of the test almost 6 grams of particles have settled. 5.32 grams was registered at 20 hours from the initiation of the test.

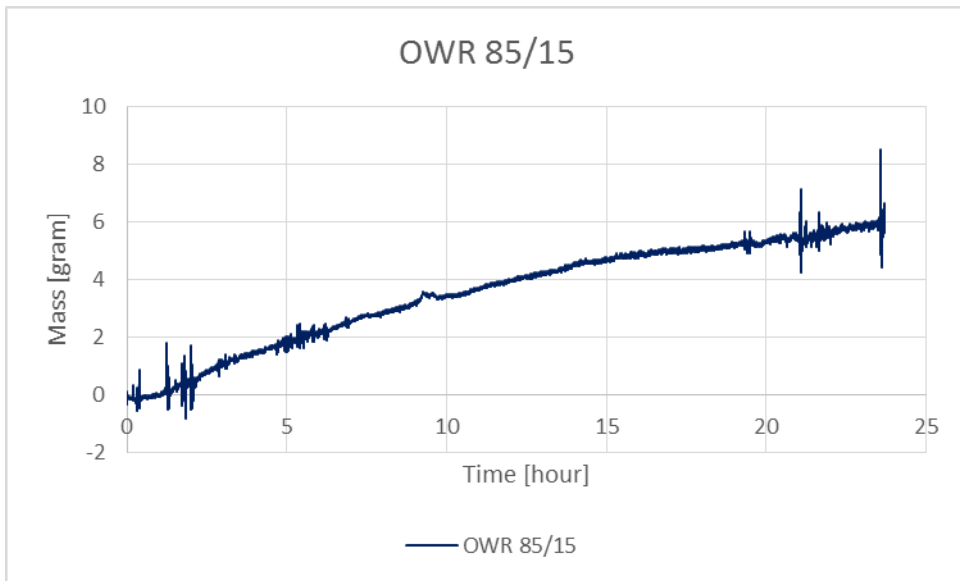


Figure 20: The curve represents the recorded weight of settling weighting particles plotted versus time.

4.3.4.2. UCA

Fig. 21 shows the results from the UCA experiment performed on Halliburton OBM with OWR 85/15. The transit time decreases rapidly the first minutes of the test. Then the curve makes a little peak around four hours after the test started. At time equal to 7 hours the transit time starts to increase after being stable for 2 hours, and continues to increase for the entire test period. The test temperature was 35°C.

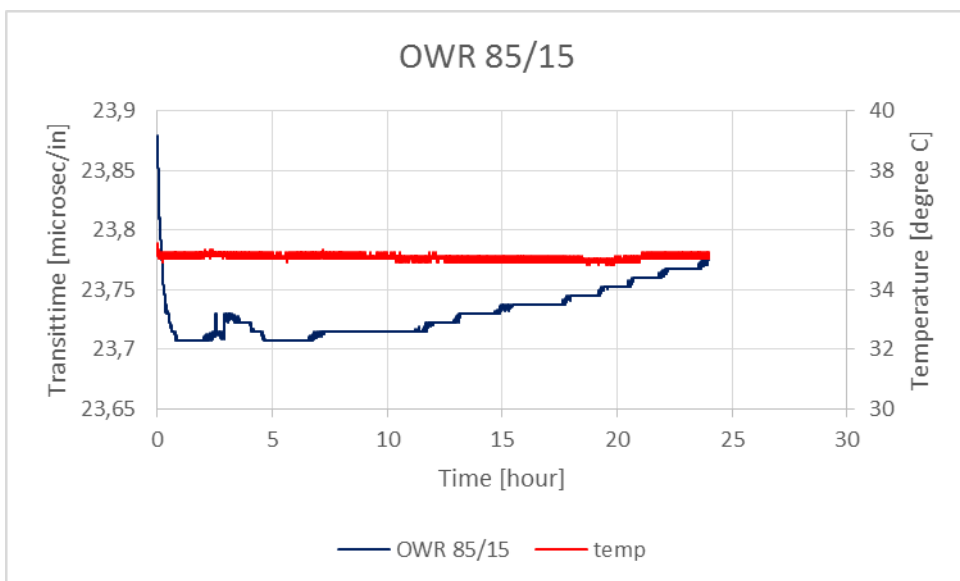


Figure 21: Transit time and temperature as a function of time.

4.3.4.3. NMR

4.3.4.3.1. 1D Profile

Fig. 22 shows the 1D profile curves for the first hour and the last hour of the test plotted together. The Y-axis is the sample column height where the bottom equals 0 cm and the top equals 6 cm. The X-axis is the NMR signal amplitude. The continuous (blue) line is the 1D profile for the beginning of the first hour and the dotted (red) line is the 1D profile after 24 hours. A clear peak can be seen at the top of the sample after 24 hours. For the bottom a drop was observed after 24 hours. One observe an increasing response from top to bottom for both profiles.

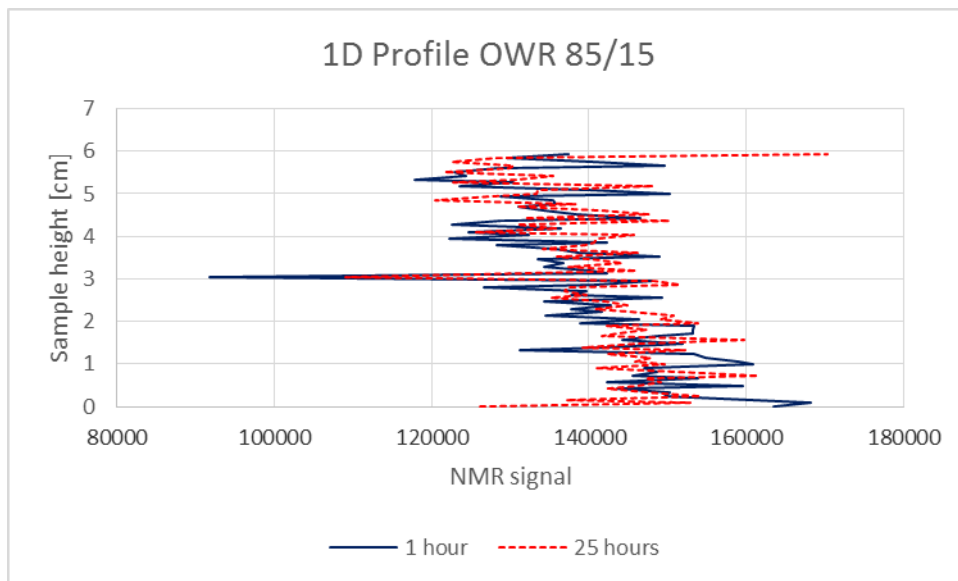


Figure 22: 1D profile of Halliburton OBM with OWR 85/15.

4.3.4.3.2. T2

Fig. 23 shows the data distribution for the relaxation time T2, for mud with OWR 85/15. The main peak in the figure shows a deviation from the trend of the previous T2 experiments. The signal strength is higher and the distribution is narrower than for the mud with 75 and 80% oil.

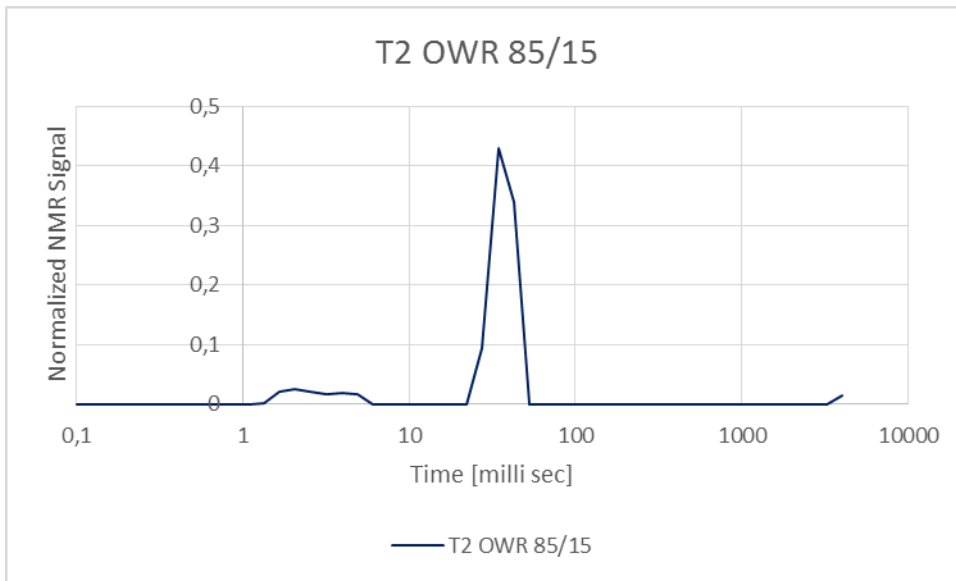


Figure 23: *T2 relaxation time distribution data for Halliburton OBM with OWR 85/15.*

4.3.5. Summarized results of direct weight measurement

The results from the direct weight measurement tests performed on Halliburton OBM are summarized in Table 5. The table presents the registered amount of weight material that has settled after 20 hours.

Table 5: *Recorded weight in the direct weight apparatus of settling weight particles after 20 hours for Halliburton OBM.*

| OWR | Recorded weight of settling particles after 20 hours [gram] |
|--------------|---|
| 70/30 | 3.38 |
| 75/25 | 3.27 |
| 80/20 | 4.89 |
| 85/15 | 5.32 |

4.3.6. Geometric Mean T2 Relaxation Time

The Geometric mean of the T2 relaxation time was calculated for the Halliburton OBM with different OWR. Fig. 24 shows the oil fraction plotted against the geometric mean of the T2 relaxation time for each fluid. The X-axis is in milli seconds, and the Y-axis is oil fraction. The text boxes in the figure indicates the OWR for each point. A straight line is drawn between each point. The curve indicates an exponential relationship between the oil fraction and the T2 relaxation time of the fluid. The T2 relaxation time increases with increased oil fraction. Even if the curve of the Fourier transformed T2 echoes showing the relaxation time distribution in Fig. 23 is breaking the pattern compared to the other curves, the Geometric mean of the relaxation time seems to fit the other data in Fig. 24.

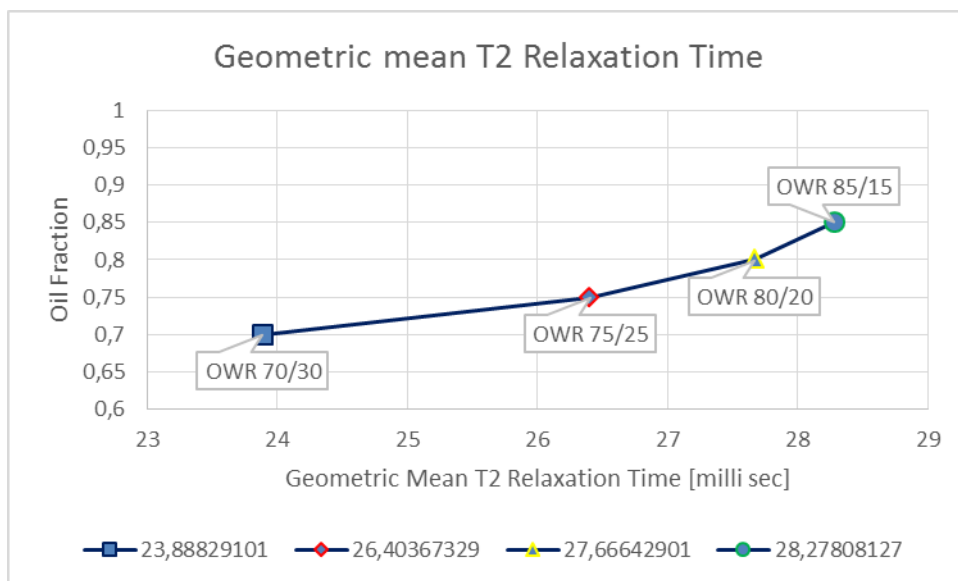


Figure 24: Geometric mean of the T2 relaxation time for Halliburton OBM.

4.4. Rheology

Rheology, Electric Stability test (ES) and mud weight of the Halliburton OBM is listed in Table 6. One can see from the results that the viscosity of the mud is decreasing with increasing oil content. The results from the ES indicates that there is not much change in the stability of the mud at different OWR. The test performed on OWR 75/25 gave the highest value, while the other values were practically the same. From the mud weight measurements one can see the effect from increasing the oil content and decreasing the water content on the different OWR. The measured values seem to be a little high compared to the calculated value for OWR 75/25. Rheology measurements and ES was performed at 50 °C. Mud weight was measured at room temperature ≈ 21°C.

Table 6: Fluid properties of Halliburton OBM.

| OWR | 70/30 | 75/25 | 80/20 | 85/15 |
|------------------------|--|-------|-------|-------|
| RPM | Shear stress [lbf/100ft ²] | | | |
| 600 | 70.8 | 53.4 | 41.2 | 41.6 |
| 300 | 39.1 | 29.7 | 24.1 | 22.3 |
| 200 | 26.9 | 22.4 | 17.9 | 16.1 |
| 100 | 14.8 | 13.2 | 11.1 | 9.9 |
| 6 | 1.9 | 2.4 | 2.4 | 3.3 |
| 3 | 1.5 | 2.2 | 2.1 | 2.4 |
| PV | 31.7 | 24.0 | 17.2 | 17.4 |
| YP | 7.3 | 5.8 | 5.2 | 4.8 |
| Gel strength 10 sec | 2.1 | 2.6 | 2.7 | 2.4 |
| Gel strength 10 min | 2.5 | 2.8 | 3.2 | 3.0 |
| ES [Volt] | 1020 | 1420 | 1020 | 1060 |
| Mud weight [SG] | 1.75 | 1.70* | 1.72 | 1.70 |

* Calculated value in accordance to mud additives

5. Discussion

Due to a comparatively high water content, the direct weight measurement test performed on OWR 70/30 was expected to show the least sag. By comparing the results from the direct weight measurement tests performed on all four different OWRs there is a clear trend indicating this is true. There is a deviation from the expectation on the test performed on OWR 75/25. This might just be due to the high stability of the drilling fluid. It might seem like the sag potential is unaffected by the change of oil ratio from 0.7 to 0.75.

5.1. OWR 70/30

The result from the direct weight measurement fits the expectations from Halliburton of this mud having a low sag potential. By comparison to the UIS mud, the recorded sag of 3.38 g after 20 hours for this mud shows that this drilling fluid is very stable regarding suspension of the weight particles.

By looking at the result from the UCA test presented in Fig.9 one can see that the difference in maximum and minimum transit time during the whole test was about 0.025 microsec/in., where the maximum value was 23.1 and the minimum value was 23.075. The start value of about 23.13 is not considered, as the sudden steep and large deflection may possibly be caused by temperature variations at the beginning of the test. One can see that the change in transit time is biggest in the beginning and gets smaller towards the end of the test. This can possibly be due to the fact that the change in the fluid phase is biggest in the start when the amount of settling particles is highest. If that is so, one might actually be able to interpret the amount of barite sag by the amplitude of the deflection in measured transit time.

The result from the 1D profile in Fig. 10 shows very little difference from the 1. hour of the test and to the 24.th hour measurement. Both curves show an increasing value towards the bottom of the tube, and the signal strength is more or less the same for both measurements.

5.2. OWR 75/25

The result from the direct weight measurement test is indicating that the rate of settling have not changed much in comparison to the test performed on drilling fluid with OWR 70/30. In fact, the results shows that there have been less settling after increasing the OWR. Two more direct weight measurement tests performed on the test fluid with OWR 75 /25 indicates that the result is not far off. Therefore, it may just seem like the sag potential of the particular drilling fluid has not changed with the increase in OWR. The tests not presented in the text can be found in the appendix.

The curve in Fig. 13 shows that the difference between the maximum and minimum transit time for this test was about 0.035 microsec/in. That is without taking into account the start value, and by interpreting the maximum value as 23.2 and the minimum value as 23.165 from the figure. We now see that the difference between max and minimum value has increased about 0.01 compared to the test performed on OWR 70/30, where the amount of sag measured on the direct weight measurement was about the same. The transit time in general are also higher than in the test on OWR 70/30.

From the 1D profile shown in Fig. 14 one can see that the NMR signal strength increases from top to bottom in this case as well. The difference between top and bottom is highest for the measurement performed after 24 hours. Three cm above the bottom of the sample there is registered a peak at both the first and the last measurement. When the 1D profile experiment is performed, a gradient field is set up. At a certain time, the frequency of the external field will be equal to the Larmor frequency of the proton spin in the fluid. This will create a signal with maximum visibility. This might be just what the peak is showing.

5.3. OWR 80/20

In this case, it is clear that the rate of settling has increased in comparison to the test performed on Halliburton OBM with lower OWR. After 20 hours, the measured weight of the settled particles are 4.89 grams, which equals about 1.50 grams increase compared to the other OWRs.

The result from the UCA test performed on Halliburton OBM with OWR 80/20 are seen in Fig. 17. The cycle of decreasing transit time, followed by an increase in transit time before the transit time again decreases seen in this case looks much like what was seen for the mud with lower OWR. For OWR 75/25, the transit time started to increase at the end, after approximately 17 hours. In this case, it can be seen from Fig. 17 that each period of the cycle takes less time and that the transit time starts to increase again after only 10 hours. By looking at the direct weight measurement test shown in Fig. 16 one can see that after 10 hours the recorded weight of the settling particles was about 3 grams. In the direct weight measurement test performed on the mud with OWR 75/25, it can be seen that the weight of the accumulated weighting material was about 3 grams after approximately 17 hours. The increasing transit time seen towards the end of the tests may possibly be interpreted as the effect of the sediment bed building up at the bottom of the test cell.

The 1D profile for OWR 80/20 in Fig. 18 shows a phenomenon that has not been seen in the tests with lower OWR. There is a signal peak at the top of the sample after 24 hours. Regarding a study published by Rismanto (2007) this might be interpreted as pure liquid (oil) due to the effect of syneresis.

5.4. OWR 85/15

As expected the fluid with the highest OWR show the most sag. It can look like it might take longer time before the maximum recorded weight is reached compared to the tests performed on mud with lower OWR.

From all tests performed on the UCA it is clear that the transit time is higher when the OWR is higher. The trend of the recorded transit time seems to follow the same pattern for all tests. For the case with OWR 85/15 the transit time shifts from decreasing to increasing after approximately 7 hours. This is the time when the accumulated weight of the weighting particles reaches approximately 3 grams in the direct weight measurement test performed on the mud with OWR 85/15. This result is supporting the theory that the increase towards the end of the test may be due to accumulation of sediments at the bottom of the cell.

In Fig. 22 one can again see what may be interpreted as syneresis at the top of the sample. As before the curves are almost inseparable with an increasing NMR signal towards the bottom of the sample. In this case however, the measurement after 24 hours show that the signal at the bottom is lower than at the first measurement. According to Rismanto (2007) this may be interpreted as solids accumulation at the bottom of the tube. The direct weight measurement test shows in this case that the weight of the settled weighting material after 20 hours was 5.32 grams. This corresponds to an increase in 2 grams compared to the samples with the least sag. Hence, the fluid with the highest sag potential fits the expectations based on previous studies. This might suggest that it is hard to interpret any effect of sag by the use of NMR if the sag potential is small.

5.5.T2

The relaxation time distribution for the T2 measurements seems to spread out as the OWR is increasing. This might have to do with a spread in the dephasing process of the proton spin, due to a different contribution from the relaxation mechanisms. The suspended microbarite particles are treated to become less water wet, hence the suspended particles are preferably in contact with the oil-phase in the mud. The fluid in contact with grains have a shorter relaxation time due to the effect of surface relaxation as mentioned previously. As the oil ratio increases in the mud, one might think that the contribution from the surface relaxation would increase since the weighting particles in the mud has a preferentially oil wet surface. The effect of increasing the amount of weighting particles in the mud while keeping the OWR the same, would possibly give the same kind of response.

The increasing spread of the T2 relaxation time with increasing OWR might also have a relation to the emulsion stability of the mud. Regarding the 1D profile experiments, there seems to be an increase in free layer fluid at the top of the test samples with increasing OWR. This might be due to increased amount of expelled fluid due to increased sag, and it may have to do with separation of the oil and water phase in relation to emulsion in-stability.

6. Conclusion

Measurements performed using an UCA on mud with four different OWRs shows that the transit time is higher for higher OWR.

Mud viscosity is decreasing with increasing OWR.

The formation of a sediment bed due to weighting material sag can probably be detected as a continuous steady increase in transit time.

For the specific mud used in this study, the transit time went from decreasing to increasing at the time equal to approximately 3 grams of weighting material sag at the bottom of the cell, without regard to OWR.

The NMR 1D profile measurements shows indications of sag for the mud sample with the most sag. This sample has approximately 5.32 grams of settled weighting material after 20 hours.

It might be hard to interpret sag from 1D profile measurements if the sag potential is low.

The geometric mean of the T2 relaxation time for the Halliburton OBM seem to fit an exponential curve, increasing with increasing OWR.

The relaxation time distribution for the T2 experiments seems to increase with increasing OWR.

References

- Bamberger, J. A. G. (2004). "Using ultrasonic attenuation to monitor slurry mixing in real time." Ultrasonics 42: 145-148.
- Bern, P. A. Z., M. Slater, K.S. Hearn, P.J. (1996). "The Influence of Drilling Variables on Barite Sag." SPE 36670.
- Boycott, A. E. (1920). "Sedimentation of Blood Corpuscles." Nature 104.
- Cheng, J. (2005). "NMR Surface relaxation, Wettability and OBM drilling fluids." (Thesis submitted in partial fulfilment of the requirements for the degree Doctor of Philosophy, RICE University).
- Coates, G. X., L. Prammer, M. (1999). "NMR Logging Principles & Applications." (Halliburton Energy Services, Houston).
- Dye, W., et al. (1999). "Correlation of Ultra-Low Shear Rate Viscosity and Dynamic Barite Sag in Invert-Emulsion Fluids." SPE 56636(Presented at the SPE ATCE, Houston, 3-6 Oct.).
- Egeland, C. (2009). "Investigation of structural breakdown of drillingfluids by imposed vibration."
- Jamison, D. E. M., R.J. (2003). "Apparatus and method for analysing well fluid sag." 6, 584, 833.
- Lambert, J. B. M., E.P. (2004). "Nuclear Magnetic Resonance Spectroscopy." (Pearson Education Inc).
- Mitchell, R. F. M., Stefan Z. (2011). "Fundamentals of Drilling Engineering." SPE Textbook Series 12.
- Mjøhus, S. (2011). "Particle sedimentation detection using an ultrasonic cement analyser."
- Omland, T. H. (2009). "Particle Settling in non-Newtonian Drilling Fluids."
- Omland, T. H. A., Tron. Taugbøl, Knut. Saasen, Arild. Svanes, Kåre. Amundsen, Per Amund. (2004). "The Effect of the Synthetic- and Oil-Based Drilling Fluids Internal Water-Phase Composition on Barite Sag." SPE 87135.
- Omland, T. H. S., Arild. Amundsen, Per A. (2007). "Detection Techniques Determining Weighting Material Sag in Drilling Fluid and Relationship to Rheology." Annual Transactions of the Nordic Rheology Society 15.
- Omland, T. H. S., Arild. Amundsen, Per A. Hodne, Helge. Mjøhus, Stian. (2010). "Rig-site equipment determines drilling fluid weight material sag." Oil and Gas Journal.

Omland, T. H. Ø., Jorun. Svanes, Kåre. Saasen, Arild. Jacob, Hans-Joachim. Sveen, Terje. Hodne, Helge. Amundsen, Per A. (2004). "Weighting Material Sag." Annual Transactions of the Nordic Rheology Society 12.

Rismanto, R. V. d. S., Claas. (2007). "Explorative Study of NMR Drilling Fluids Measurement." Annual Transactions of the Nordic Rheology Society 15.

Saasen, A. L., D. Marken, C.D. Sterri, N. Halsey, G.W. Isambourg, P. (1996). "Prediction of Barite Sag Potential of Drilling Fluids from Rheological Measurements." SPE/IADC 29410.

Taugbøl, K. F., G. Prebensen, O.I. Svanes, K. Omland, T.H. Svela, P.E. Breivik, D.H. (2005). "Development and Field Testing of a Unique High- Temperature/High- Pressure (HTHP) Oil- Based Drilling Fluid With Minimum Rheology and Maximum Sag Stability." SPE 96285.

Tehrani, A. P., A. Ayansina, T. (2009). "Barite Sag in Invert-Emulsion Drilling Fluids."

Zamora, M. (2009). "Mechanisms, Measurement and Mitigation of Barite Sag."

Appendix A: Fig. A1-A25

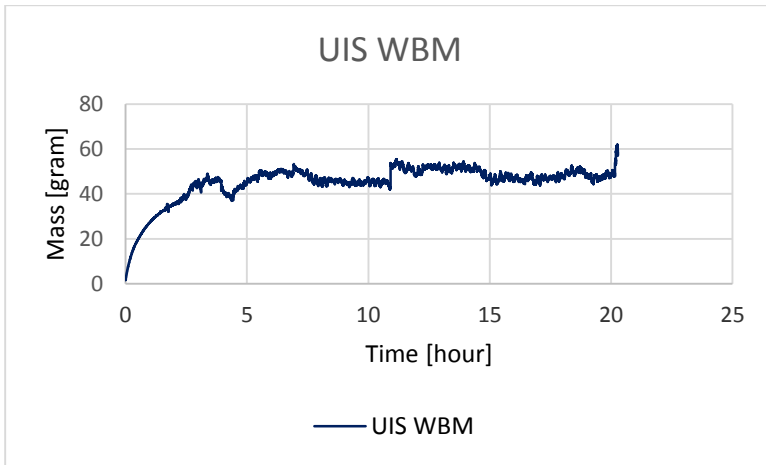


Figure A1: Direct weight measurement of UIS WBM

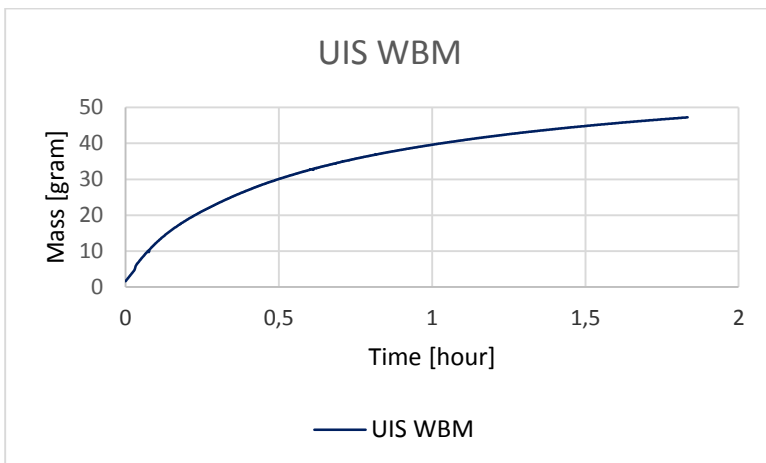


Figure A2: Direct weight measurement of UIS WBM

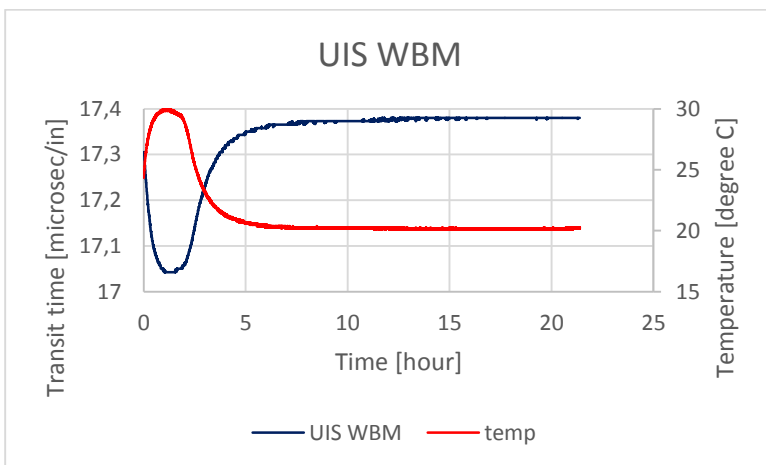


Figure A3: UCA experiment performed on UIS WBM

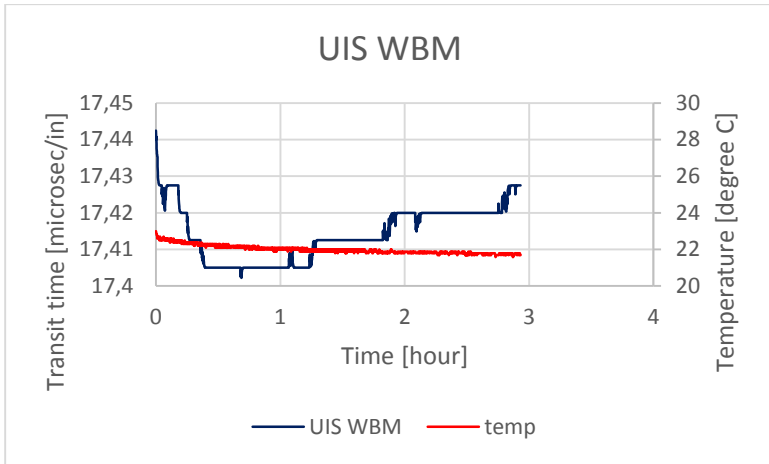


Figure A4: UCA experiment performed on UIS WBM

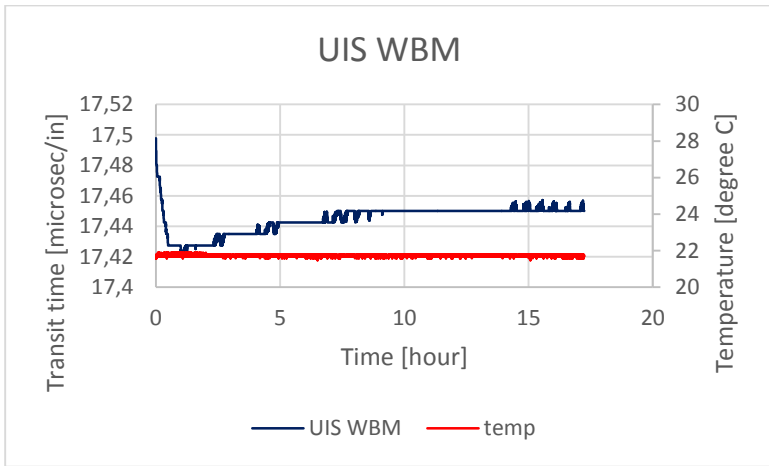


Figure A5: UCA experiment performed on UIS WBM

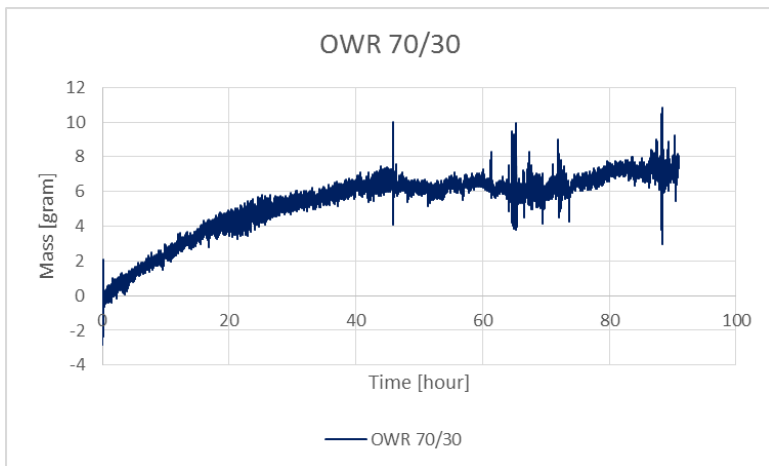


Figure A6: Direct weight measurement of Halliburton OBM with OWR 70/30

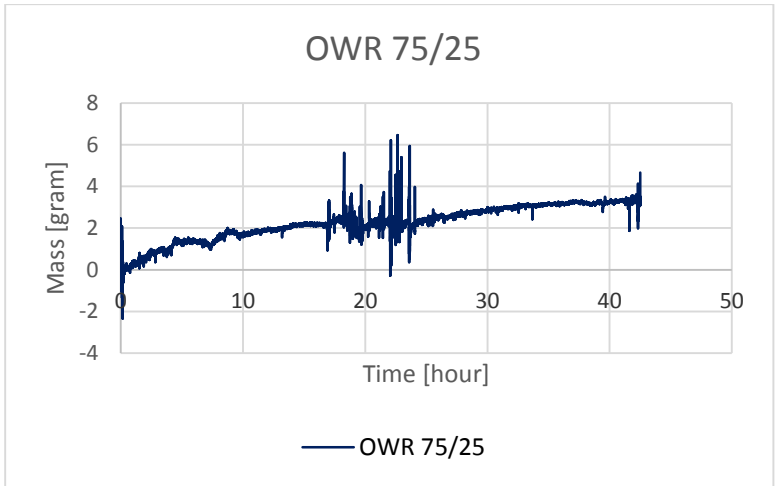


Figure A7: Direct weight measurement of Halliburton OBM with OWR 75/25

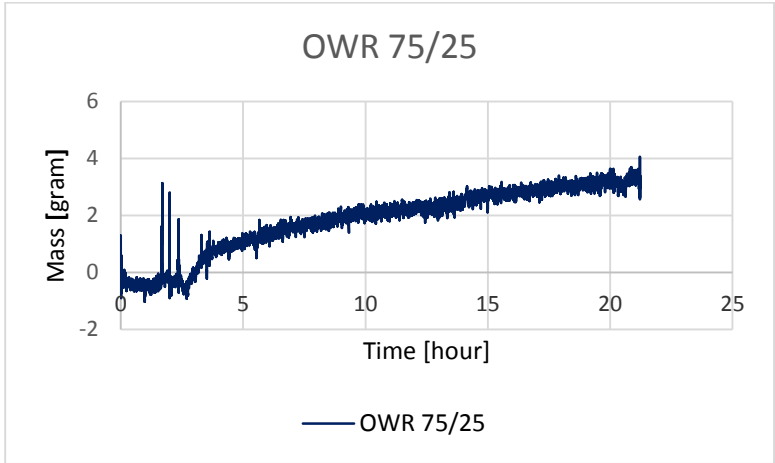


Figure A8: Direct weight measurement of Halliburton OBM with OWR 75/25

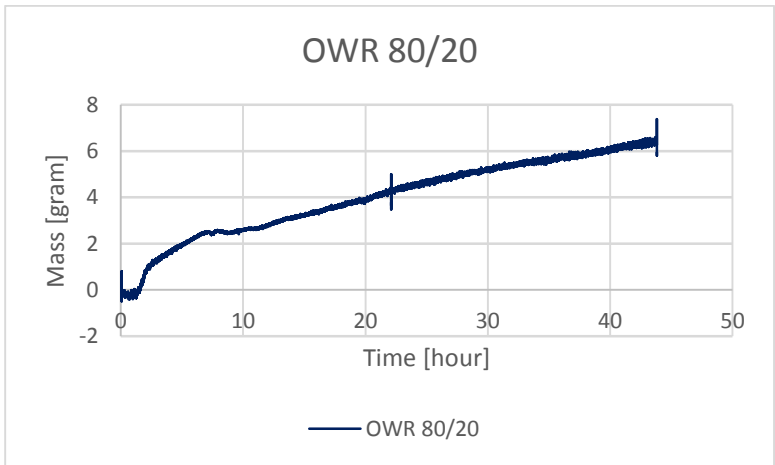


Figure A9: Direct weight measurement of Halliburton OBM with OWR 80/20

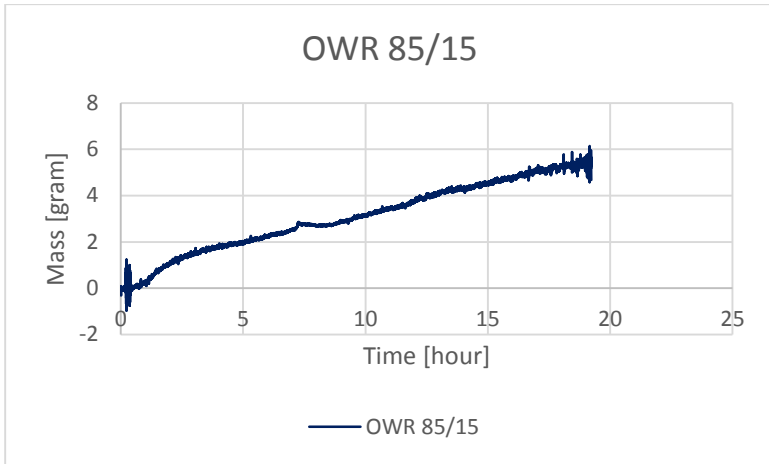


Figure A10: Direct weight measurement of Halliburton OBM with OWR 85/15

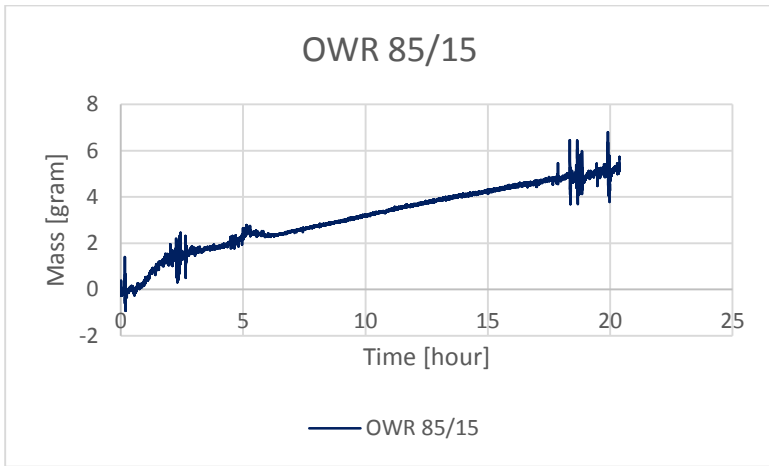


Figure A11: Direct weight measurement of Halliburton OBM with OWR 85/15

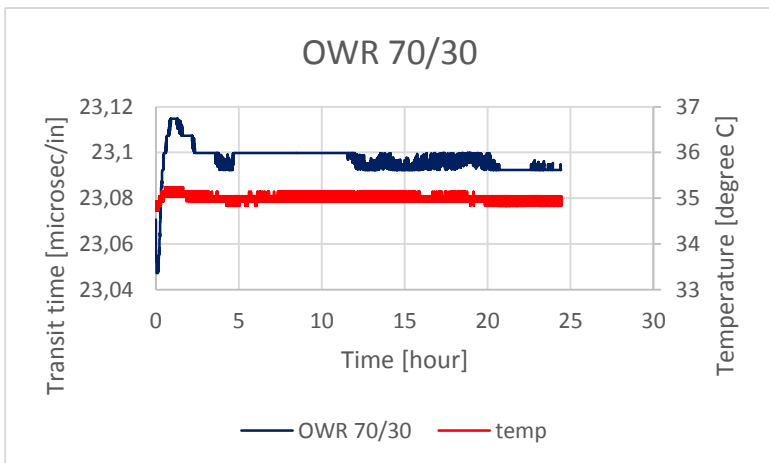


Figure A12: UCA experiment performed on Halliburton OBM with OWR 70/30

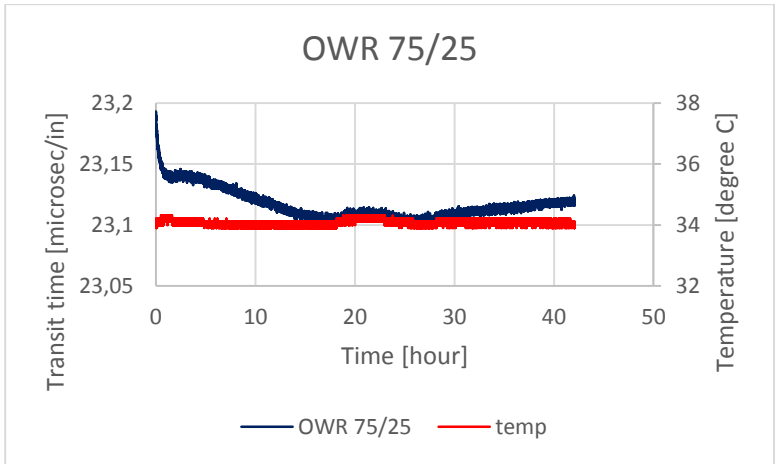


Figure A13: UCA experiment performed on Halliburton OBM with OWR 75/25

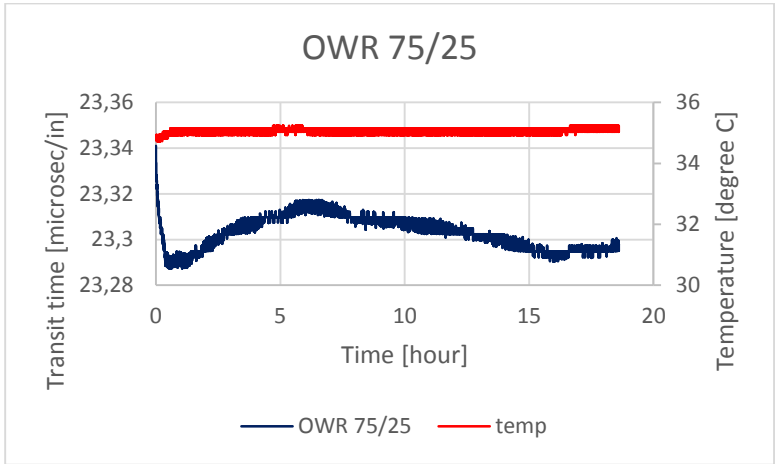


Figure A14: UCA experiment performed on Halliburton OBM with OWR 75/25

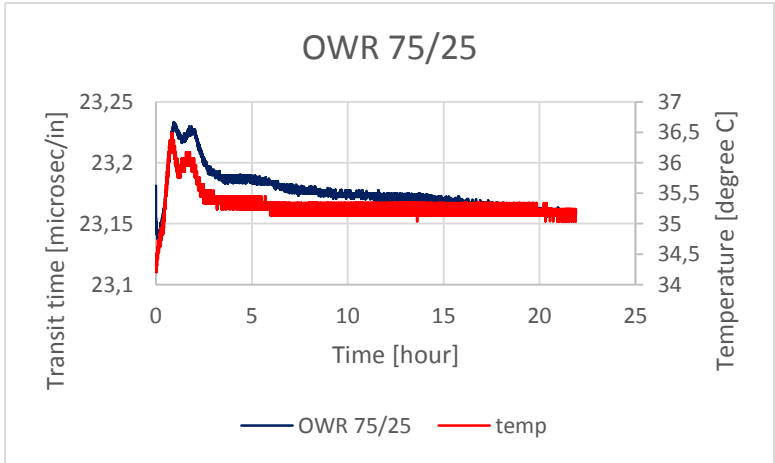


Figure A15: UCA experiment performed on Halliburton OBM with OWR 75/25

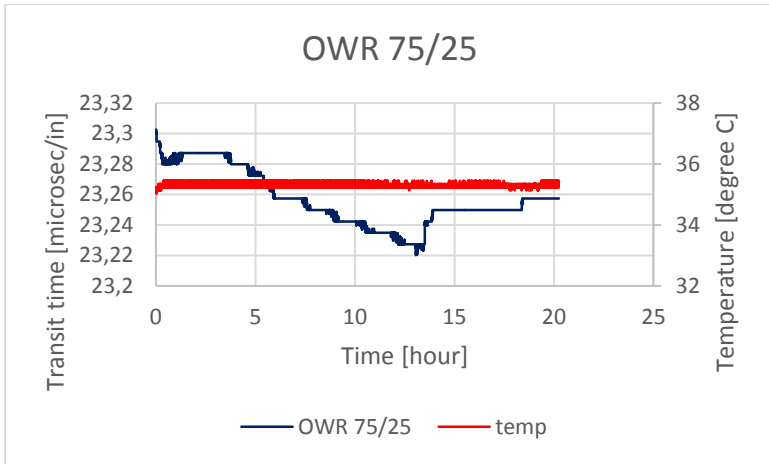


Figure A16: UCA experiment performed on Halliburton OBM with OWR 75/25

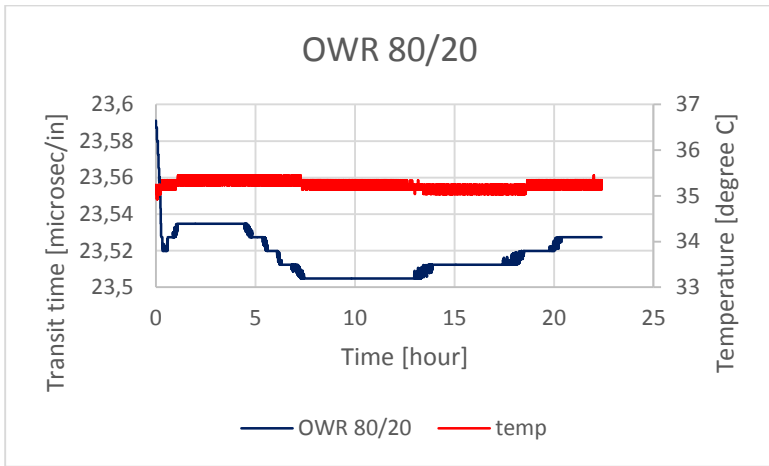


Figure A17: UCA experiment performed on Halliburton OBM with OWR 80/20

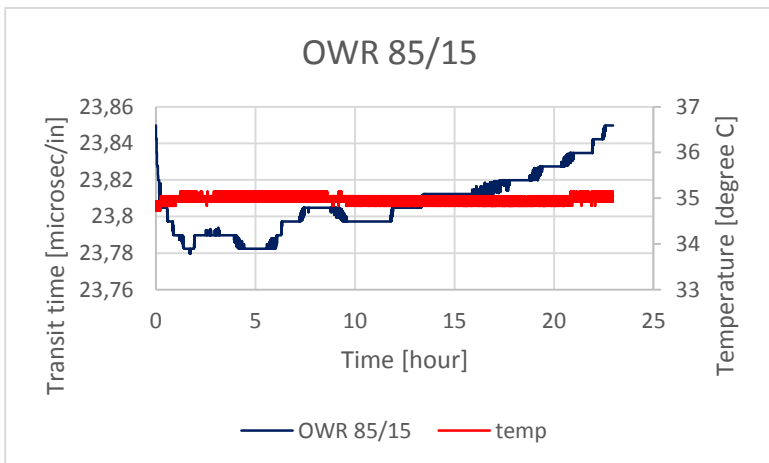


Figure A18: UCA experiment performed on Halliburton OBM with OWR 85/25

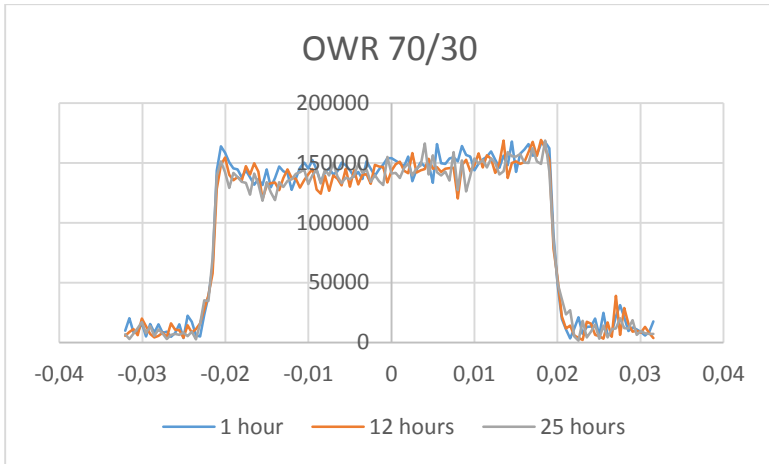


Figure A19: 1D profile experiment on Halliburton OBM with OWR 70/30

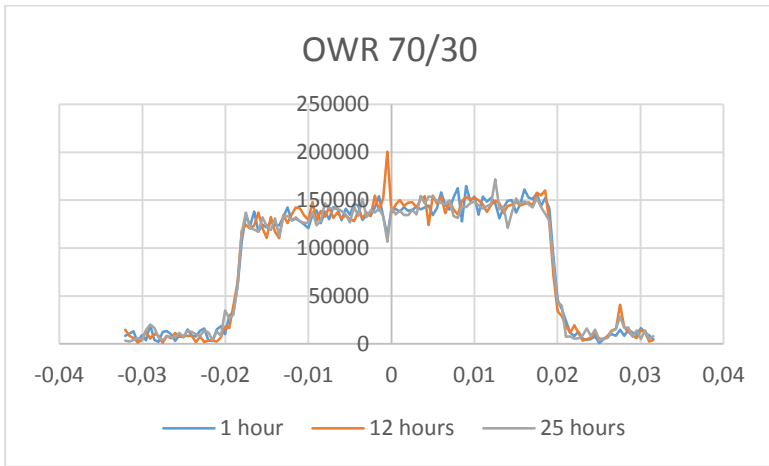


Figure A20: 1D profile experiment on Halliburton OBM with OWR 70/30



Figure A21: 1D profile experiment on Halliburton OBM with OWR 75/25

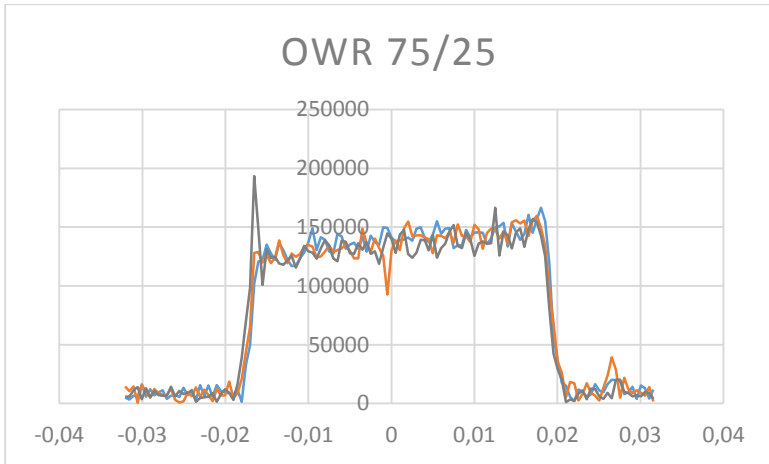


Figure A22: 1D profile experiment on Halliburton OBM with OWR 75/25

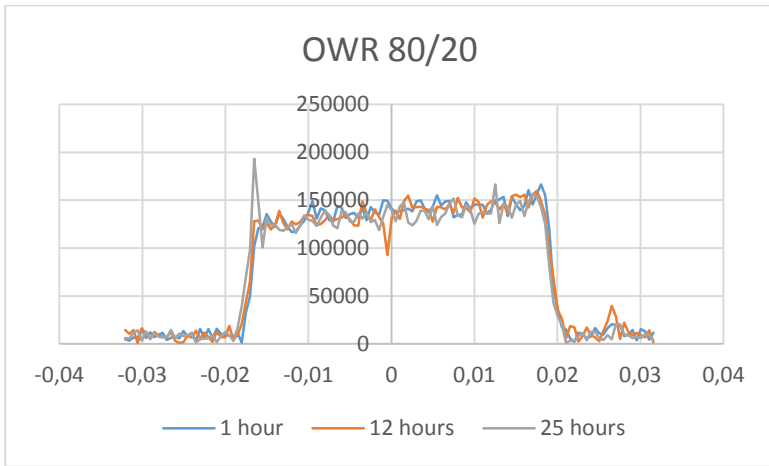


Figure A23: 1D profile experiment on Halliburton OBM with OWR 80/20

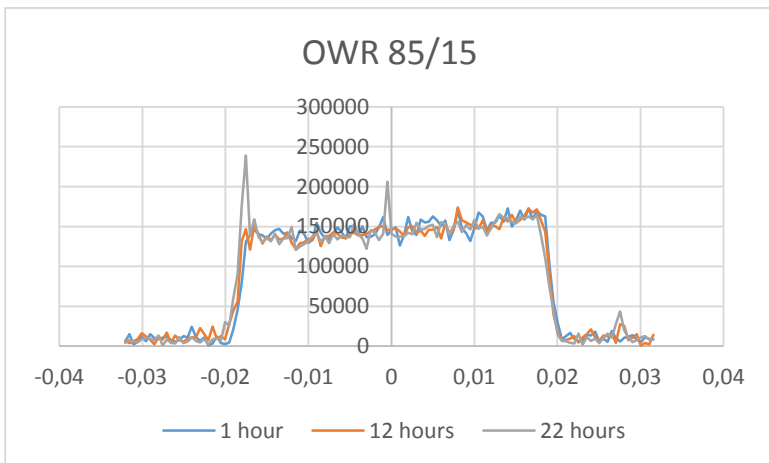


Figure A24: 1D profile experiment on Halliburton OBM with OWR 85/15

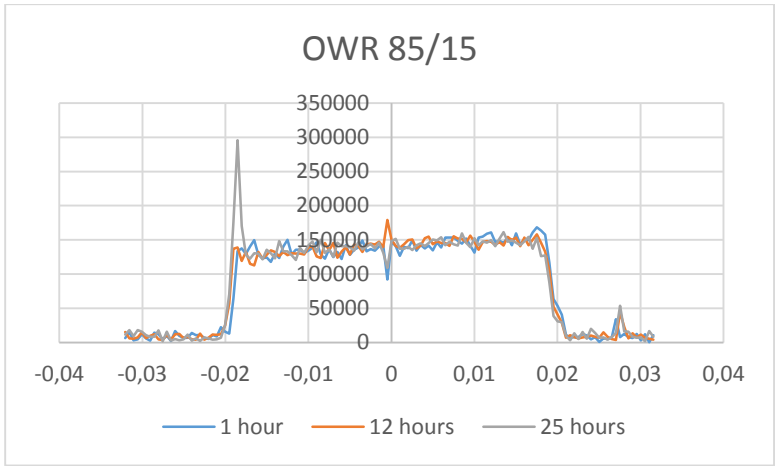


Figure A25: 1D profile experiment on Halliburton OBM with OWR 85/15

Appendix B: Formula for calculating geometric mean of the T2 relaxation time

$$T2 \text{ geometric mean} = e^{\sum(\text{normA} * \ln t)}$$

Where normA is normalized NMR signal amplitude and t is the relaxation time in millisec.

Appendix C: NMR script for T2 measurements and 1D profile experiments

```
Option Explicit

Dim DataName_Con

dim starttime, endtime, tottime, waittime, runtime
dim i
dim CurDir
dim ExpDir
dim fso
dim aout
dim txt0
sub main()
' waittime = 360 - 300
' NMR.StatusMessage("WAIT "& waittime )
'   NMR.EXECUTE("WAIT " & waittime)

'end sub
'sub test

DataName_Con = GetDataName(2)
If DataName_Con="" Then           ' Empty string if <Cancel> pressed
Exit Sub
End If

CurDir=NMR.GetParameter("%DATADIR")   ' Get current data directory
ExpDir=NMR.GetParameter("%DATADIR")

Set fso=CreateObject("Scripting.FileSystemObject")
Set aout = fso.CreateTextFile(DataName_Con & ".txt",true)

aout.WriteLine("Czas pomiaru: " & Date & " " & Time )
aout.WriteLine("Pomiar: " & DataName_Con)
aout.WriteLine(txt0)
aout.WriteLine(" ")
for i = 1 to 25
```

```

starttime = timer
T2
T2Plot
profile
endtime = timer
tottime = endtime - starttime
waittime = 3600 - totime

NMR.EXECUTE("WAIT " & Cln(waittime))

'runtime = timer
'Do while runtime > 300
'  wait
'  endtime = timer
'  totime = endtime - starttime
'Loop

next

end sub

' T2 subroutine
sub T2

DoAutoO1

'Måling av CPMG
NMR.StatusMessage(" Running T2")
NMR.EXECUTE("~AMODE")
NMR.EXECUTE("LOAD CPMG")
NMR.EXECUTE("FW 100000")
NMR.EXECUTE("DW 1")
NMR.EXECUTE("SW 1000000")
NMR.EXECUTE("SI 1")
NMR.EXECUTE("NECH 2048")
NMR.EXECUTE("NS 16")
NMR.EXECUTE("RG 100")

```

```

NMR.EXECUTE("RD 6S")
NMR.EXECUTE("TAU 250")

Nmr.Go                                ' Starter Cpmg målinga
'Lagring av data:

NMR.Execute("WR " & DataName_Con & "_T2_" & "raw_NS" & "16_" & i & " Y")

' Comment out save of Excel data for T2 measurement Ola Ketil Sigveland
'NMR.Execute("EX " & DataName_Con & "_T2_" & "raw_NS" & "16_" & i)

End Sub

'***** End T2 Måling *****

'***** Start T2Plot *****

Sub T2Plot

Dim X_T2,X_a, X_b, X_Chi, X_StdEr
Dim Stid, Etid, TotTid, NaaTid, minTid, SekTid
Stid = timer

NMR.Execute("T2 F")
X_T2= Nmr.getparameter("%R0")
X_a= Nmr.getparameter("%R1")
X_b= Nmr.getparameter("%R2")
X_chi= Nmr.getparameter("%R3")
X_StdEr= Nmr.getparameter("%R4")

aout.WriteLine(" T2 plott with result data ms ")
aout.WriteLine("      T2 = " & X_T2 & " ms ")
aout.WriteLine("      a = " & X_a & " init amplitude")
aout.WriteLine("      b = " & X_b & " offset")
aout.WriteLine("      Chi = " & X_chi & " Chi square")
aout.WriteLine("Std err = " & X_StdEr & " Standard error on fit")
aout.WriteLine(" ")

'Tidsmåling
Etid = Timer

```

```

TotTid = Etid - Stid
Naatid = Time
if totTid > 60 then
mintid = int(totTid/60)
SekTid = tottid - (minTid*60)

aout.WriteLine("T2 Plott godzina: " & NaaTid & " pomiar zajal: " & minTid & " min, "&
sekTid & " sek")

else

aout.WriteLine("T2 Plott godzina: " & NaaTid & " pomiar zajal: " & TotTid & " Sec")

end if

aout.WriteLine(" ")

End Sub

!***** End T2Plot *****

'1D profile subroutine
sub profile

'Måling av CPMG
NMR.EXECUTE("~AMODE")
NMR.EXECUTE("LOAD PROFILE")
NMR.EXECUTE("DEAD1 60")
NMR.EXECUTE("DEAD2 15")
NMR.EXECUTE("FW 100000")
NMR.EXECUTE("DW 15.6")
NMR.EXECUTE("SI 128")
NMR.EXECUTE("NS 128")
NMR.EXECUTE("RG 100")
NMR.EXECUTE("RD 10000000")
NMR.EXECUTE("TAU 4000")
NMR.EXECUTE("G1 1000")
NMR.EXECUTE("G2 1000")
NMR.EXECUTE("PH1 02")
NMR.EXECUTE("PH2 02")
NMR.EXECUTE("PH3 11")

NMR.StatusMessage("Running 1D profile no: " & i)

```

```
Nmr.Go                                ' Starter Cpmg målinga
'Lagring av data:

NMR.Execute("WR " & DataName_Con & "1D_" & "raw_NS" & "16_" & i & " Y")
NMR.Execute("EX " & DataName_Con & "1D_" & "raw_NS" & "16_" & i)

NMR.Execute("FT")
NMR.Execute("MAG")

NMR.Execute("WR " & DataName_Con & "1D_" & "FT_MAG_NS" & "16_" & i & " Y")
NMR.Execute("EX " & DataName_Con & "1D_" & "FT_MAG_NS" & "16_" & i)

End Sub
'***** End profile Måling *****
```